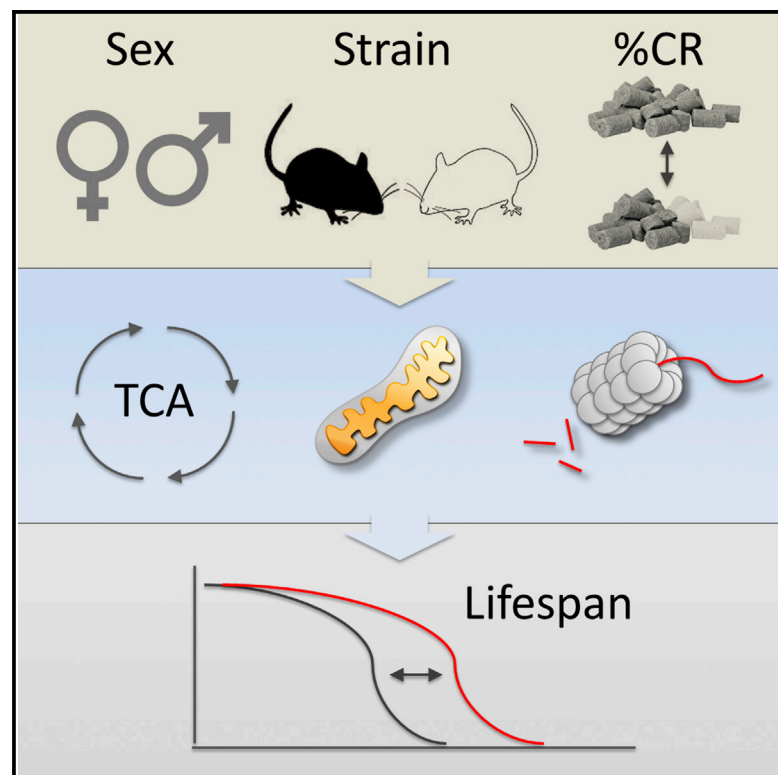


Cell Metabolism

Effects of Sex, Strain, and Energy Intake on Hallmarks of Aging in Mice

Graphical Abstract



Authors

Sarah J. Mitchell,
Julio Madrigal-Matute,
Morten Scheibye-Knudsen, ...,
Donald K. Ingram, Michel Bernier,
Rafael de Cabo

Correspondence

decabora@mail.nih.gov

In Brief

In this paper Mitchell et al. systematically addresses sex- and strain-dependent responses to various levels of caloric restriction. Notably, caloric restriction universally increases health span through maintenance of energy metabolism and proteostasis with aging. However, there are strain/sex-dependent differences in lifespan extension by caloric restriction, perhaps uncoupling health span and lifespan.

Highlights

- Caloric restriction (CR) prevents the age-related decline in proteostasis
- Mitochondrial function is necessary for lifespan extension through CR
- Health and survival outcomes are separated in response to CR in mice
- The CR response depends on strain, sex, and level of CR

Accession Numbers

GSE81959



Effects of Sex, Strain, and Energy Intake on Hallmarks of Aging in Mice

Sarah J. Mitchell,¹ Julio Madrigal-Matute,² Morten Scheibye-Knudsen,^{1,3,4} Evandro Fang,³ Miguel Aon,⁵ José A. González-Reyes,⁶ Sonia Cortassa,⁵ Susmita Kaushik,² Marta Gonzalez-Freire,¹ Bindi Patel,² Devin Wahl,¹ Ahmed Ali,¹ Miguel Calvo-Rubio,⁶ María I. Burón,⁶ Vincent Guitierrez,¹ Theresa M. Ward,¹ Hector H. Palacios,¹ Huan Cai,⁷ David W. Frederick,⁸ Christopher Hine,⁹ Filomena Broeskamp,¹⁰ Lukas Habering,¹⁰ John Dawson,^{11,12} T. Mark Beasley,^{11,12} Junxiang Wan,¹³ Yuji Ikeno,¹⁴ Gene Hubbard,¹⁴ Kevin G. Becker,¹⁵ Yongqing Zhang,¹⁵ Vilhelm A. Bohr,³ Dan L. Longo,¹⁵ Placido Navas,¹⁶ Luigi Ferrucci,¹ David A. Sinclair,¹⁷ Pinchas Cohen,¹³ Josephine M. Egan,⁷ James R. Mitchell,⁹ Joseph A. Baur,⁸ David B. Allison,^{11,12} R. Michael Anson,¹ José M. Villalba,⁶ Frank Madeo,¹⁰ Ana Maria Cuervo,² Kevin J. Pearson,^{1,18} Donald K. Ingram,¹⁹ Michel Bernier,¹ and Rafael de Cabo^{1,*}

¹Translational Gerontology Branch, Intramural Research Program, National Institute on Aging, NIH, 251 Bayview Boulevard, Suite 100, Baltimore, MD 21224, USA

²Department of Developmental and Molecular Biology, Institute for Aging Studies, Albert Einstein College of Medicine, Bronx, NY 10461, USA

³Laboratory of Molecular Gerontology, Intramural Research Program, National Institute on Aging, NIH, 251 Bayview Boulevard, Suite 100, Baltimore, MD 21224, USA

⁴Department of Cellular and Molecular Medicine, Center for Healthy Aging, University of Copenhagen, 2200 Copenhagen, Denmark

⁵Laboratory of Cardiovascular Science, Intramural Research Program, National Institute on Aging, NIH, 251 Bayview Boulevard, Suite 100, Baltimore, MD 21224, USA

⁶Department of Cell Biology, Physiology and Immunology, University of Córdoba, Agrifood Campus of International Excellence, ceiA3, 14071 Córdoba, Spain

⁷Laboratory of Clinical Investigation, Intramural Research Program, National Institute on Aging, NIH, 251 Bayview Boulevard, Suite 100, Baltimore, MD 21224, USA

⁸Department of Physiology, Institute for Diabetes, Obesity, and Metabolism, University of Pennsylvania, Philadelphia, PA 19104, USA

⁹Department of Genetics and Complex Diseases, Harvard University, Boston, MA 02115, USA

¹⁰Institute of Molecular Biosciences, NAWI Graz, University of Graz, and BioTechMed Graz, 8010 Graz, Austria

¹¹Department of Biostatistics, University of Alabama, Birmingham, AL 35294, USA

¹²GRECC, Birmingham/Atlanta Veterans Administration Hospital, Birmingham, AL 35294, USA

¹³Leonard Davis School of Gerontology, University of Southern California, Los Angeles, CA 90089, USA

¹⁴Barshop Institute for Longevity and Aging Studies, University of Texas Health Science Center at San Antonio, San Antonio, TX 78245-3207, USA

¹⁵Laboratory of Genetics, Intramural Research Program, National Institute on Aging, NIH, 251 Bayview Boulevard, Suite 100, Baltimore, MD 21224, USA

¹⁶Centro Andaluz de Biología del Desarrollo, and CIBERER, Instituto de Salud Carlos III, Universidad Pablo de Olavide-CSIC, 41013 Sevilla, Spain

¹⁷Department of Genetics, Harvard Medical School, Boston, MA 02115, USA

¹⁸Graduate Center for Nutritional Sciences, University of Kentucky, C.T. Wethington Building, Room 591, 900 South Limestone, Lexington, KY 40536, USA

¹⁹Pennington Biomedical Research Center, Baton Rouge, LA 70809, USA

*Correspondence: decabora@mail.nih.gov

<http://dx.doi.org/10.1016/j.cmet.2016.05.027>

SUMMARY

Calorie restriction (CR) is the most robust non-genetic intervention to delay aging. However, there are a number of emerging experimental variables that alter CR responses. We investigated the role of sex, strain, and level of CR on health and survival in mice. CR did not always correlate with lifespan extension, although it consistently improved health across strains and sexes. Transcriptional and metabolomics changes driven by CR in liver indicated anaplerotic filling of the Krebs cycle together with fatty acid fueling of mitochondria. CR prevented age-associated decline in the liver proteostasis network while increasing mitochondrial number, preserving mitochondrial ultrastructure and function with age.

Abrogation of mitochondrial function negated life-prolonging effects of CR in yeast and worms. Our data illustrate the complexity of CR in the context of aging, with a clear separation of outcomes related to health and survival, highlighting complexities of translation of CR into human interventions.

INTRODUCTION

More than a century ago, Moreschi (Moreschi, 1909) and Rous (Rous, 1914) observed the beneficial impact of a reduction of caloric intake on transplanted and induced tumors. It was years later when Osborne (Osborne et al., 1917) and then McCay and colleagues reported the lifespan effects of calorie-restricted diet in rats (McCay et al., 1935). Since then, calorie restriction (CR) has consistently shown beneficial effects on longevity,

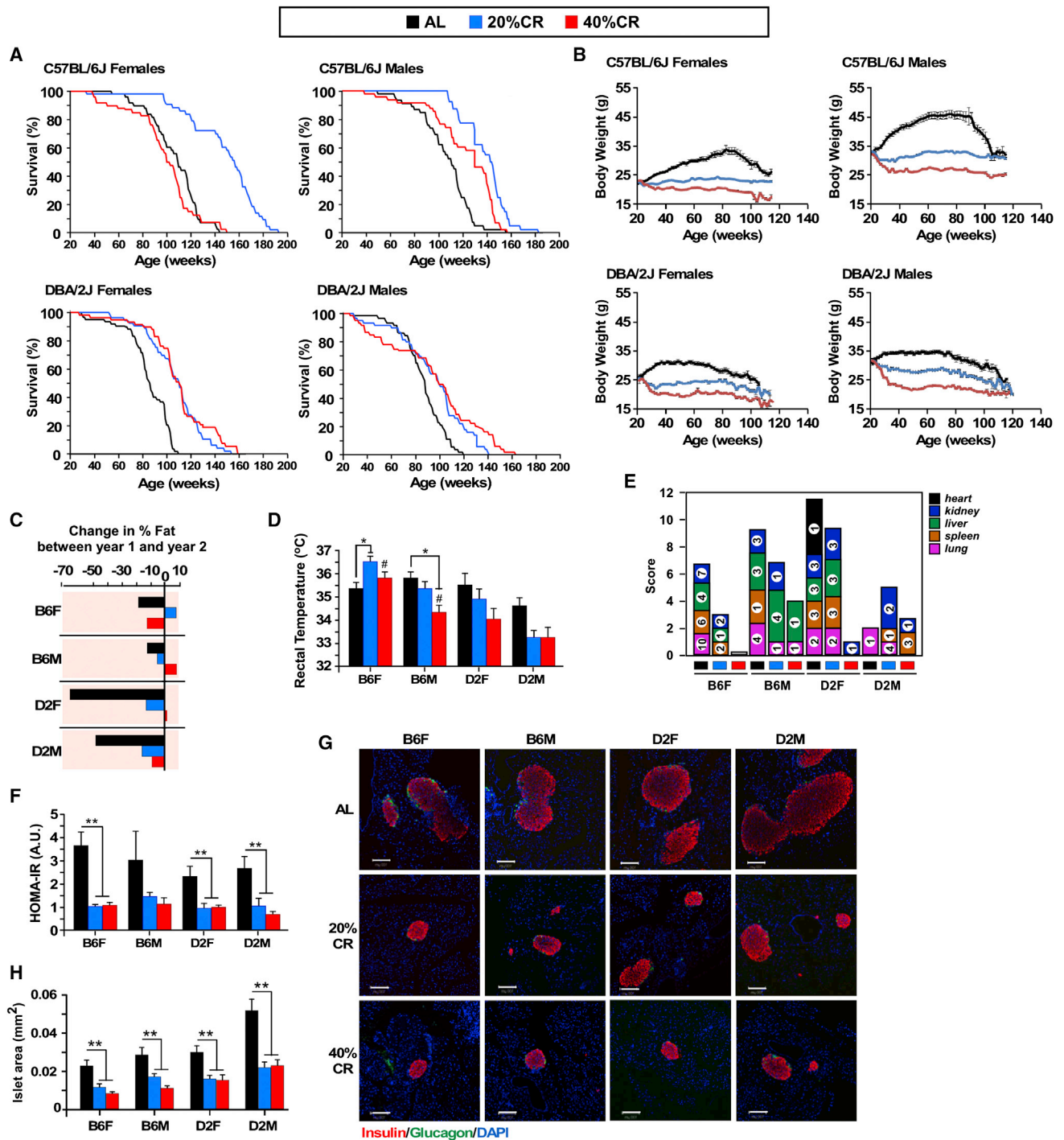


Figure 1. Sex- and Strain-Specific Effects of Caloric Restriction on Lifespan and Health Span in Mice

(A) Kaplan-Meier survival curves for mice fed either a standard diet ad libitum (AL) or maintained on 20% and 40% calorie restriction (CR). n = 50–63 mice per experimental group.

(B) Body weight trajectories of mice fed either a standard diet AL or maintained on 20% and 40% CR. n = 50–63 mice per experimental group.

(C) Change in percent fat mass measured by nuclear magnetic resonance spectroscopy between year 1 and year 2. n = 11–50 per experimental group, 11–13 months of age (5–7 months on diet) and 22–24 months of age (16–18 months on diet).

(D) Rectal temperatures measured in mice. n = 8 per experimental group, 18–19 months of age, 12–13 months on diet.

(E) Prevalence of different grade lymphomas. n = 4–12 mice per experimental group. For ages please see Table S3B.

(F) The homeostatic model assessment calculation of insulin resistance (HOMA-IR). n = 6 per experimental group, 23–24 months of age, 17–18 months on diet.

(legend continued on next page)

age-associated diseases, attenuation of functional decline, and tumorigenesis across a variety of species and diet formulations (Gross and Dreyfuss, 1984; Kritchevsky, 2002; Tannenbaum, 1940; Weindruch and Sohal, 1997; Weindruch et al., 1986). Nevertheless, the exact mechanism(s) underlying these effects remain unknown. Among the most extensively studied hallmarks of CR are enhanced protection against induced and spontaneous carcinogenesis, reduced insulin/insulin-like growth factor 1 (IGF-1) signaling, reduction in oxidative stress and/or increase in antioxidant mechanisms (De Cabo et al., 2004), decrease in different pathologies (Berg and Simms, 1960; Cheney et al., 1980; Ikeno et al., 2013), enhanced mitochondrial function (López-Lluch et al., 2006; Nisoli et al., 2005), improved proteostasis and autophagy (Cuervo, 2008; Hansen et al., 2008), a reduction in body temperature (Rikke et al., 2003), and reduction in reproductive investment (Mitchell et al., 2015b), among others. All these outcomes are accompanied by increases in median and maximum lifespan (Bartke et al., 2007; Gross and Dreyfuss, 1984; Kritchevsky, 2002; Weindruch and Sohal, 1997; Weindruch et al., 1986). These beneficial effects on health and survival have been reported even after alteration in the macronutrient content and/or restriction of specific components of the diet such as methionine or protein, different feeding regimens, and periodic periods of fasting (Fontana and Partridge, 2015; Hine et al., 2015; Masoro, 1990; Miller and Roth, 2007; Murtagh-Mark et al., 1995; Solon-Biet et al., 2015). However, recent evidence suggests that all these tenets may not always hold true. For example, CR does not increase lifespan in all mouse strains (Fernandes et al., 1976; Forster et al., 2003; Goodrick et al., 1990; Harper et al., 2006; Harrison and Archer, 1987; Liao et al., 2010, 2011; Rikke et al., 2010; Turturro et al., 2002). A remaining question is therefore what factors influence the response to CR.

Traditionally, diet composition and genetic background have been thought to have little influence on the lifespan extension by CR. Recently, data emerging from two independent non-human primate studies challenged this association by reporting similar improvements in health but contrasting survival benefits in response to CR (Colman et al., 2009; Mattison et al., 2012). This uncoupling of lifespan/health span benefits by CR has been reported in earlier studies in mice and non-human primates (Colman et al., 2009; Mattison et al., 2012; Rikke and Johnson, 2007; Turturro and Hart, 1991). The notion of a direct correlation between lifespan extension, health, and CR, regardless of the context, needs to be revisited. It is becoming clear that multiple variables should be considered before the optimal implementation of CR. Perhaps it is possible that the differential responses observed are context dependent, particularly on the interactions between diet, strain, sex, and the degree of CR imposed. We posit here that there is an “ideal” context in which CR benefits will be maximized for each individual. Using a comprehensive analysis in this study, we sought to test the impact that genetic background (strain), sex, and level of CR have on the traditional response to this intervention and to further elucidate the poten-

tial underlying mechanisms linking extension of lifespan and health in mice.

RESULTS

Effects of Strain and Sex on the Health Span and Lifespan of Mice on CR

To determine the role of strain and sex on the lifespan of mice on varying degrees of CR, female and male C57BL/6J and DBA/2J (herein referred to as B6 and D2, respectively) mice were fed Harlan 18% protein diet either ad libitum (AL) or at 20% and 40% CR starting at 6 months of age for the remainder of their lives (Figure 1A). In B6 mice, 20% CR significantly improved survival, with a mean lifespan extension of 40.6% in females and 24.4% in males relative to AL-fed controls (Table S1). However, B6 females on 40% CR did not show a beneficial response in survival compared to AL-fed controls (Table S1), and yet a modest 13.3% increase in maximum lifespan was observed (Figure 1A). B6 males did show beneficial effects of 40% CR, but not to the same degree of 20%. D2 mice exhibited 37.3% and 29.8% increases in maximum lifespan in both sexes maintained on 40% CR, respectively (Table S1), even though D2 males on 40% CR had an 18.8% reduction in first quarter (Q1) lifespan, an observation consistent with an earlier report (Forster et al., 2003). Interestingly, D2 females did not show further benefits from 20% to 40% CR. Thus, the response of these strains to CR shows a clear role of sex, strain, and level of CR on survival outcomes.

Mice on CR exhibited reductions in body weight trajectories that were not proportional to the reduction in caloric intake (AL > 20% CR > 40% CR; Figure 1B). Body composition was assessed at baseline (before the onset of CR) and at 12 and 24 months of age (Table S2). D2 males had a considerably higher percentage of body fat than D2 females and B6 mice at baseline, which they maintained throughout their life. By 12 months of age, body fat and lean mass percentages were similar across diet groups; however, strain-specific differences in body composition were apparent at 24 months of age, with CR-fed D2 mice exhibiting the greatest protection against loss in percentage body fat associated with aging (Table S2, Figure 1C). Despite being maintained on 40% CR, 24-month-old B6 females had a percentage of body fat loss similar to AL-fed controls. It is possible that the preservation of fat mass in CR mice between 12 and 24 months of age plays a protective role in survival and lifespan extension, in agreement with previous findings (Liao et al., 2011).

One of the primary physiological responses to CR is the reduction in body temperature (Weindruch et al., 1979) in rodents (Duffy et al., 1989; Mitchell et al., 2015a; Speakman and Mitchell, 2011), non-human primates (Lane et al., 1995), and humans (Soare et al., 2011). We measured rectal body temperature (T_b) during the dark cycle and found that D2 mice had generally lower T_b compared to B6 mice, with a trend toward T_b reduction with CR versus AL (Figure 1D). A stepwise reduction in T_b with increasing level of CR was observed in male B6 mice, whereas

(G) Immunofluorescence images of pancreatic islets stained for insulin (red; Texas Red), glucagon (green; FITC), and DAPI (blue, DAPI). Scale bar, 100 μ m. n = 6 per experimental group, 23–24 months of age, 17–18 months on diet.

(H) Islet area (mm^2). n = 4–6 per experimental group, 23–24 months of age, 17–18 months on diet. Bars represent mean \pm SEM. * $p < 0.05$ compared to AL; # $p < 0.05$ compared to 20% CR.

B6 females on 20% CR had a significant elevation in T_b compared to AL and 40% CR (Figure 1D).

Another characteristic feature of CR is the reduction in the type and number of pathologies (Berg and Simms, 1960; Che-ney et al., 1980; Ikeno et al., 2013). Any animal that died during the study underwent a necropsy and gross pathological examination to determine the cause of death (Table S3A). A subset of tissues underwent further histopathological analysis by a board-certified pathologist blinded to the dietary intervention (Table S3B). In general, there was a delay in the incidence of most commonly occurring pathologies (e.g., lymphoma) in response to CR, as CR-fed animals died at an older age with the same pathologies (Figure 1E, Table S3). Notably, there was a CR dose-dependent decrease in pathologies even in the groups that showed little or no lifespan extension. The incidence of other pathologies such as glomerulonephritis was unchanged across groups (Table S3B), indicating that CR can only delay the onset of age-related diseases but not fully prevent pathologies associated with aging.

CR Attenuates Age-Associated Impairments in Glucose Homeostasis and Maintains Pancreatic Islet Morphology

One of the proposed mechanisms of CR-mediated lifespan extension is the maintenance of insulin sensitivity (Barzilai et al., 1998). We measured markers of insulin sensitivity, namely circulating glucose, insulin, leptin, and adiponectin in mice either maintained on AL or on 20% or 40% CR (Table S4). Glucose and insulin levels were lower and appeared to plateau in B6 females maintained on 20% CR versus AL. While CR-fed D2 females exhibited a dose-dependent decrease in blood glucose with no changes in circulating insulin, B6 and D2 males on CR showed a stepwise reduction in glucose and insulin levels (Table S4). The homeostatic measure of insulin resistance (HOMA-IR) was significantly lower with CR across the experimental groups, plateauing at 20% CR (Figure 1F, Table S4). We measured fasting serum IGF-1 and IGFBP-1 in mice (Table S4) and found a reduction in IGF-1 levels with increasing level of CR regardless of the mouse sex or strain, which is in agreement with previous reports (Anson et al., 2003; Breese et al., 1991; Mitchell et al., 2015b). The long-term effects of CR on circulating IGFBP-1 levels are paradoxical, with increased concentrations in humans (Fontana et al., 2016), but a significant decrease in rodents when compared to AL-fed controls (Breese et al., 1991). Here, serum IGFBP-1 was higher in CR-fed D2 mice and B6 females on 40% CR, but was lower in CR-fed B6 males and B6 females on 20% CR than in their AL-fed controls (Table S4). In contrast, circulating adiponectin was higher and leptin was lower with both degrees of CR than in the AL-fed groups regardless of mouse strain and sex (Table S4). CR was associated with a dose-dependent increase in adiponectin levels relative to AL-fed mice, except for B6 females where adiponectin levels plateaued with 20% CR. Circulating levels of leptin were reduced in B6 mice on CR, consistent with a recent report (Mitchell et al., 2015b). Notably, leptin levels were much lower in the AL-fed D2 females than in all other groups of mice on AL, consistent with the fact that D2 female mice had the lowest percentage of body fat mass (Table S2). Leptin levels are negatively correlated with level of CR in B6 male mice (Mitchell et al.,

2015b). This was consistent with our study (data not shown) in both male and female B6 mice, but not D2 mice, highlighting the complexity in the physiological response to CR across different strains of mice.

To further investigate glucose homeostasis, we examined pancreatic islet area and found a significant reduction in 17- to 23-month-old mice on CR compared to AL-fed controls (Figures 1G and 1H). The ratio in the number of α/β cells was significantly lower with CR, indicating that the process of islet hypertrophy that occurs as a consequence of aging (Figueroa and Taberner, 1994) appears to be ameliorated with CR independent of mouse strain and sex.

Transcriptional Profiling of the Effect of Varying Degrees of CR on Liver Gene Expression

The liver is essential for the maintenance of metabolic homeostasis and the resulting energetic balance of the organism. Therefore, to further define the pathways and genes that were affected by CR, we performed whole-genome microarray analysis on liver samples of 2-year-old male and female B6 and D2 mice. Principal component analysis (PCA) showed a clear effect of strain (PC1) and CR (versus AL feeding; PC2) on liver transcriptome for both females (Figure 2A) and males (Figure 2B). To understand the determinants responsible for the unique lifespan trajectories in response to CR, four-way Venn diagrams were plotted with the four CR20-AL (Figures 2C and 2D) and CR40-AL (Figures 2F and 2G) pairwise comparisons. The number of transcripts that were upregulated (Figures 2C and 2F) and downregulated (Figures 2D and 2G) are depicted, with more than 262 shared transcripts (139 upregulated and 123 downregulated) in response to 20% CR and 290 shared transcripts (141 upregulated and downregulated) with 40% CR as compared to AL-fed littermates. Parametric analysis of gene set enrichment enabled the identification of significantly altered gene sets in the CR20-AL, CR40-AL, and CR40-CR20 pairwise comparisons, and these included the upregulation of pathways implicated in fatty acid metabolism, mitochondrial bioenergetics, and phase II conjugation and the downregulation of gene sets associated with genome integrity, transcription, and inflammation (Figures 2E and 2H). Canonical pathways related to fatty acid metabolism and the top 20 CR-regulated transcripts in the four CR40-CR20 pairwise comparisons are depicted in Tables S5A and S5B, respectively. Figure 2I depicts a binary representation of gene expression related to mitochondrial electron transport chain among all 24 pairwise comparisons, where the effect of diet, mouse strain, and sex was evaluated. Similar representation of gene expression related to fatty acid metabolism and core components of nucleosome is shown in Figure S1. Another important effect observed in the analysis of these data was the downregulation by CR of major urinary proteins (MUPs), consistent with a reduction in their reproductive capacity (Figure S1C). This family of proteins is directly linked to reproduction and the energetic switch between reproduction and somatic protection (Kirkwood, 2002). The decrease in MUPs observed herein with CR is consistent with recently published data in B6 males (Mitchell et al., 2015b). In our study, these effects were more pronounced in males than females, particularly in B6 mice, suggesting that CR may lead to somatic sparing while sacrificing reproductive fitness.

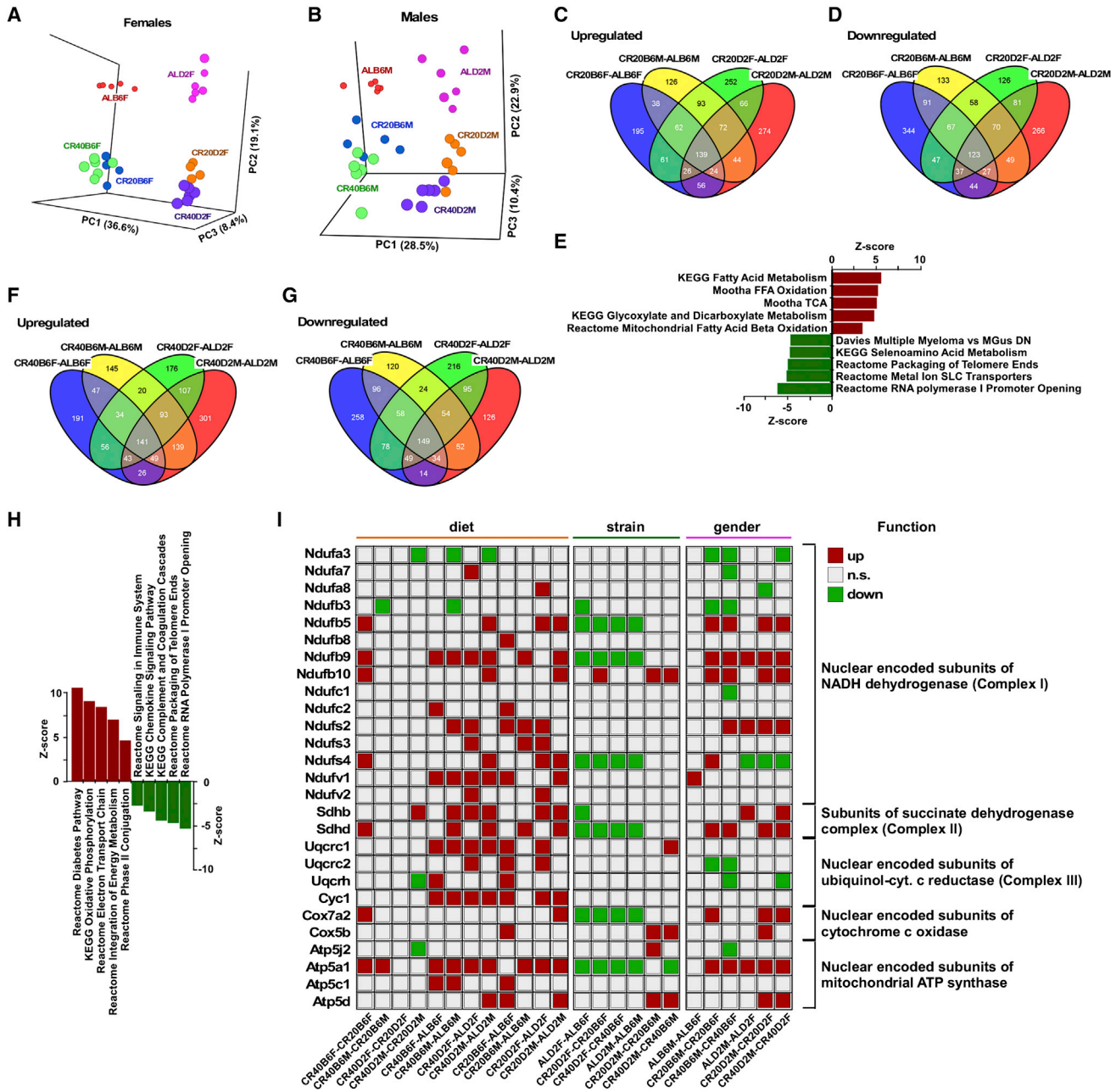


Figure 2. Impact of Mouse Strain and Sex in the Global Hepatic Gene Expression Profile of Mice Fed CR versus AL

(A and B) PCA scatterplot analysis revealed the impact of mouse strain (PC1) and diet (AL versus 20% and 40% CR) (PC2) in female and (B) male mice. The difference in pattern between 20% CR and 40% CR was modest, especially in B6 females (PC3). CR40B6F, B6 females on 40% CR; CR40D2F, D2 females on 40% CR; CR20D2F, D2 females on 20% CR; CR40B6M, B6 males on 40% CR; CR20B6M, B6 males on 20% CR; CR40D2M, D2 males on 40% CR; CR20D2M, D2 males on 20% CR.

(C and D) Four-way Venn diagrams of upregulated (C) and downregulated (D) gene transcripts present in CR20B6F-ALB6F, CR20B6M-ALB6M, CR20D2F-ALD2F, and CR20D2M-ALD2M pairwise comparisons.

(E) Partial list of top gene sets shared among the four CR20-AL pairwise comparisons, with the Z score values of CR20B6F-ALB6F depicted.

(F and G) Four-way Venn diagrams of upregulated (F) and downregulated (G) gene transcripts present in CR40B6F-ALB6F, CR40B6M-ALB6M, CR40D2F-ALD2F, and CR40D2M-ALD2M pairwise comparisons.

(H) Partial list of top gene sets shared among the four CR40-AL pairwise comparisons, with the Z score values of CR40B6F-ALB6F depicted.

(I) Binary representation of gene expression related to mitochondrial electron transport chain among all 24 pairwise comparisons. Upregulated, red squares; downregulated, green squares; not significant, beige squares. Listing of the shared gene sets is provided in the [Supplemental Information](#). All microarray data are n = 6 biological replicates per experimental group, 23–24 months of age, 17–18 months on diet.

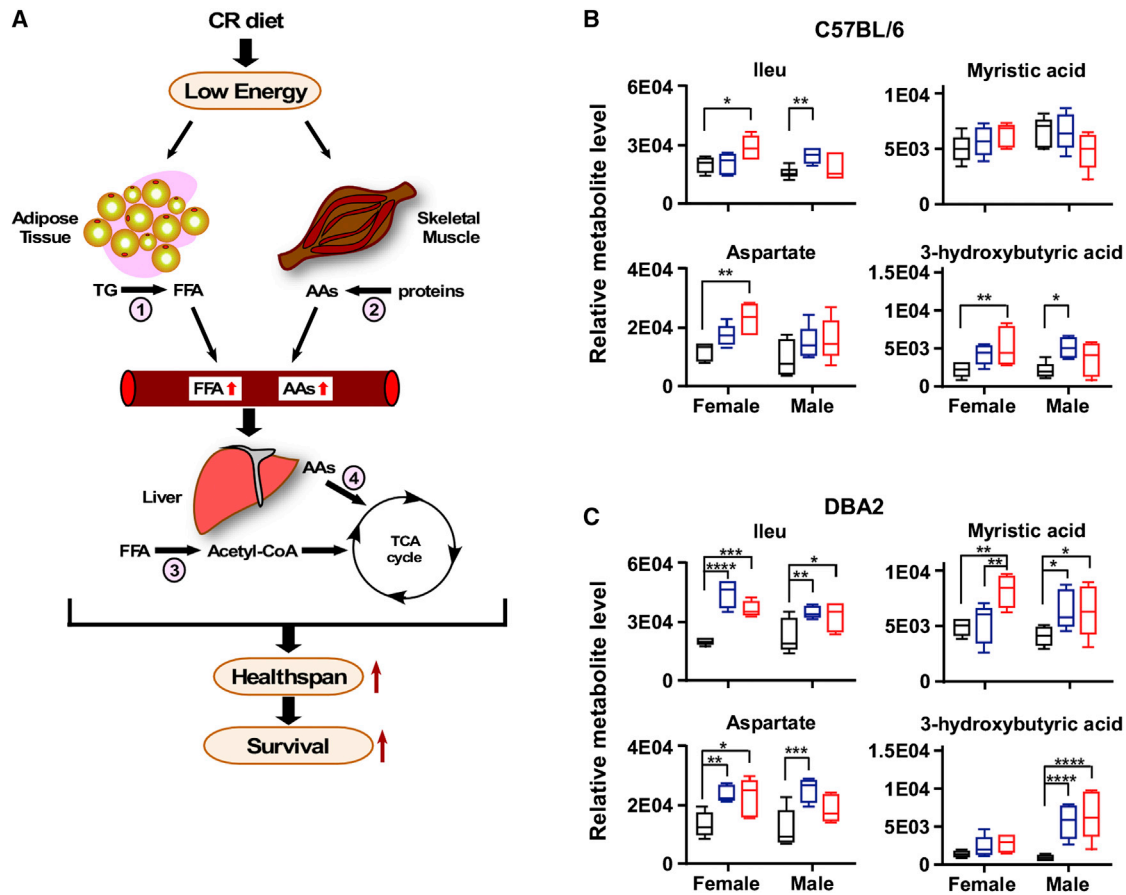


Figure 3. Metabolite Profiles in Liver of Mice on CR Indicate the Predominance of Catabolic Modes

(A) Schematic representation of the effect of CR on the release of FFA from adipose tissue (lipolysis, 1) and breakdown of proteins from skeletal muscle (ubiquitin/proteolysis and autophagy, 2), resulting in accumulation of metabolites feeding the TCA cycle in liver mitochondria (fatty acid β -oxidation, 3; anaplerotic filling of the TCA cycle via amino acids, 4). This metabolism switch could account for the increase in health span and lifespan observed in CR-fed animals.

(B and C) Relative level of Ileu, aspartate, myristate, and 3-hydroxybutyrate in B6 (B) and D2 (C) mouse liver is depicted as boxplots ($n = 6$ per group). All data are $n = 6$ biological replicates per experimental group, 23–24 months of age, 17–18 months on diet. AL, black box; 20% CR, blue box; 40% CR, red box. * $p < 0.01$, ** $p < 0.001$, *** $p < 0.05$.

Metabolomics and the Catabolic Mode of Liver Metabolism under CR

The effect of CR on metabolite profiles in the livers of D2 and B6 mice was characterized, with more than 149 metabolites identified. These were grouped by metabolic signatures (e.g., energy components, fatty acids, vitamins, etc.), and their profiles were compared between all 12 groups of mice. As an amphibolic organ, the liver can function both catabolically and anabolically. Under these conditions, the anaplerotic filling (replenishing) of the TCA cycle together with the energetic fatty acid fueling of mitochondria suggests less metabolic reliance on glucose (Figure 3A). Consequently, we interrogated the metabolite profiles for predominance of catabolic or anabolic modes during CR regimens. The profile of metabolites feeding the TCA cycle showed accumulation in CR over AL groups depending on strain and sex as could be judged by the analysis of metabolites' ratio (CR20/AL and CR40/AL) (Figures 3B and 3C). Interestingly, two-way ANOVA of metabolite levels enabled us to distinguish between the clear-cut effect of CR in D2 versus B6 strain, as can be judged from the non-significant interaction between CR and

sex in D2 mice (Table S6, Figure S2A). This result suggests a dependence of the effects of CR on the strain genetic background.

There was accumulation of a remarkably wide range of amino acids, ketogenic (e.g., Phe, Tyr, Ileu) and gluconeogenic (e.g., Gly, Thr, Asp, Met), including branched-chain (BCAAs, Val, Ileu, Leu) and essential (e.g., Val, Ileu, Leu, Lys, Met, Phe, Thr) amino acids (Figure S2B). The levels of most common circulating fatty acids were significantly enhanced as well, such as palmitic, oleic, myristic, stearic, and linoleic, along with glycerol, which represents the backbone of triacylglycerols. Other metabolites substantially elevated were glutamate, glutamine, 3-hydroxybutyrate (a ketone body), and intermediaries of the TCA cycle such as citrate, malate, and fumarate. Ornithine and fumarate accretion are in agreement with activation of the urea cycle to also feed the TCA cycle with fumarate (Figure S2B). In summary, these data support the notion that CR leads to mobilization of peripheral energy deposits that the liver can subsequently utilize for gluconeogenesis.

Hydrogen Sulfide and the Control of Protein Handling Systems

Hydrogen sulfide (H₂S) production via the transsulfuration pathway is an evolutionarily conserved response to CR that may mediate multiple CR-like benefits, including stress resistance and longevity (Hine et al., 2015). We found a dose-dependent hepatic production of H₂S across B6 and D2 mice in response to CR (Figures 4A and 4B). A heat map generated from metabolomics analysis of liver samples was used to communicate relationships between the 12 experimental groups and six major metabolites implicated in the transsulfuration pathway. Clear strain- and sex-specific differences in the patterns of changes in metabolite levels were observed (Figure S3A). The ability of CR to promote elevated levels of hepatic H₂S production was consistent with previous findings (Hine et al., 2015) and may represent a global effect of CR in inducing stress resistance.

The beneficial effects of H₂S on cellular aging may be mediated through the transcription factor Nrf2 and Cyp2a5 detoxification (Abu-Bakar et al., 2007; Chattopadhyay et al., 2012; Yang et al., 2013). Indeed, CR significantly increased *Cyp2a5* mRNA levels independently of mouse strain and sex (Figure 4C), consistent with the H₂S results.

Like CR, H₂S increases lifespan in *C. elegans* (Miller and Roth, 2007) and promotes redox regulation of SIRT1 (Zee et al., 2010) to help maintain the circadian rhythm of mouse hepatocytes (Shang et al., 2012). In our study, SIRT1 protein levels were found to be reduced with 20% CR in B6 females, but remained largely unaffected in other groups except for the significant increase in D2 males on 40% CR (full immunoblot images depicted in Figure S3B, quantitative analysis in Figure 4D, n = 6). Poly(ADP-ribose) polymerase 1 (PARP-1), a nuclear DNA repair enzyme that consumes NAD⁺, was significantly reduced with CR (exception of D2 females on 40% CR) (Figure 4D, Figure S3B). Although PARP-1 activity was not measured, it is possible that CR-induced changes in PARP-1 expression will impact on the NAD⁺ levels, thereby affecting protein deacetylation performed by sirtuins, and ultimately shape nuclear-mitochondrial communication and the control of energy homeostasis (Cantó et al., 2015; Gomes et al., 2013; Guan and Xiong, 2011). We observed that CR hindered to a certain extent the age-related reduction in hepatic NAD⁺ level, although it did not reach statistical significance (Figure 4E). Consistent with the report of Schwer et al. (Schwer et al., 2009), the global pattern of lysine acetylation and deacetylation in liver lysates was refractory to CR-mediated protein deacetylation (Figure 4D, Figure S3B), as evidenced by the fact that the ratio of acetylated to total p53 was significantly increased with CR (Figure 4D, Figure S3B). The acetylation ratio of SOD2 differed in relation to sex and strain, with 20% and 40% increases in B6 males and D2 females, respectively, which is similar to their lifespan increases with CR. The increase in SOD2 acetylation level at steady-state occurred despite higher expression of the deacetylase SIRT3 in CR samples (Figure 4F, Figure S3C). These results are consistent with CR-mediated inhibition of SIRT3 and are at odds with previous reports (Qiu et al., 2010; Tauriainen et al., 2011). Alternatively, acetylation changes could be caused by increase in acetyl-CoA levels in the liver, a phenomenon that is known to occur with fasting.

NAD(P)H:quinone oxidoreductase 1 (NQO1), a key player in the antioxidant and detoxification pathways, is a Nrf2 target protein inducible by H₂S (Chattopadhyay et al., 2012). We found that CR treatment caused a dose-dependent increase in NQO1 protein levels irrespective of sex and strain; however, the magnitude of this increase was much lower in D2 males on 40% CR (Figure 4G, Figure S3D). NQO1 also functions as a gatekeeper protein capable of competing with the 20S proteasome for interaction with different proteins (Moscovitz et al., 2015). Binding of NQO1 to the key metabolic regulator, PGC-1 α , leads to its stabilization and protection against proteasomal degradation (Adamovich et al., 2013). Here, we found a trend toward higher PGC-1 α levels in response to CR, consistent with PGC-1 α stabilization—as a consequence of NQO1 induction—and subsequent increase in the levels of mitochondrial transcription factor A (TFAM) (Figure 4G, Figure S3D). Of significance, the size and density of mitochondria were found to be significantly higher in response to CR (see below, Figure S6B). Although refractory to CR, the acetyl-CoA carboxylase (ACC) levels showed a clear dependence on sex and strain, whereas AMPK levels trended toward higher expression with CR (Figure 4G, Figure S3D), in support of an AMPK-mediated increase in mitochondrial fatty acid oxidation. FOXO3a is a downstream target of AMPK that has a role in stress resistance, glucose metabolism, and apoptosis; FOXO3 levels mirrored those of AMPK protein (Figure 4G, Figure S3D). The deficiency in thioredoxin-interacting protein (TXNIP) causes the disruption of the fasting-feeding metabolic transition (Sheth et al., 2005) and whole-body energy metabolism (DeBalsi et al., 2014). Here, TXNIP protein expression pattern increased with the degree of CR in all groups except for D2 males on 20% CR (Figure 4H, Figure S3D). Taken together, these data illustrate the contribution of sex and strain to the altered metabolism and promotion of stress resistance by CR, which, in turn, confer health and lifespan benefits.

CR and the Regulation of the Ubiquitin-Proteasome Pathway and Autophagy

The effects of sex and strain on CR-induced changes in major protein degradation systems, which include the ubiquitin-proteasome pathway and autophagy, were explored. Attachment of ubiquitin molecules to proteins is commonly used for their degradation by the 26S proteasome complex (when using the ubiquitin K48-linkage) or by autophagy (if ubiquitin chains are attached through K63-linkage) (Ciechanover, 2005; Olzmann and Chin, 2008; Tan et al., 2008). We measured the degree and type of protein ubiquitination in liver homogenates by immunoblot analysis and found that CR induced clear reduction in K48- and K63-linked ubiquitination of soluble proteins, especially in males (Figures 5A and 5B). Changes in levels of soluble ubiquitinated proteins upon CR were minimal for the two female groups, and DBA females displayed considerably higher levels of both soluble ubiquitinated proteins and also constitutive accumulation of higher-molecular-weight polyubiquitinated protein aggregates (depicted as “Agg” in Figures 5A and 5B). Although the observed changes could be a result of differences in the rate of ubiquitination, since cells can cope with proteotoxicity of misfolded proteins by increasing their aggregation or their degradation, we hypothesized that the reduction in ubiquitinated proteins observed in the male groups upon CR could reflect enhanced

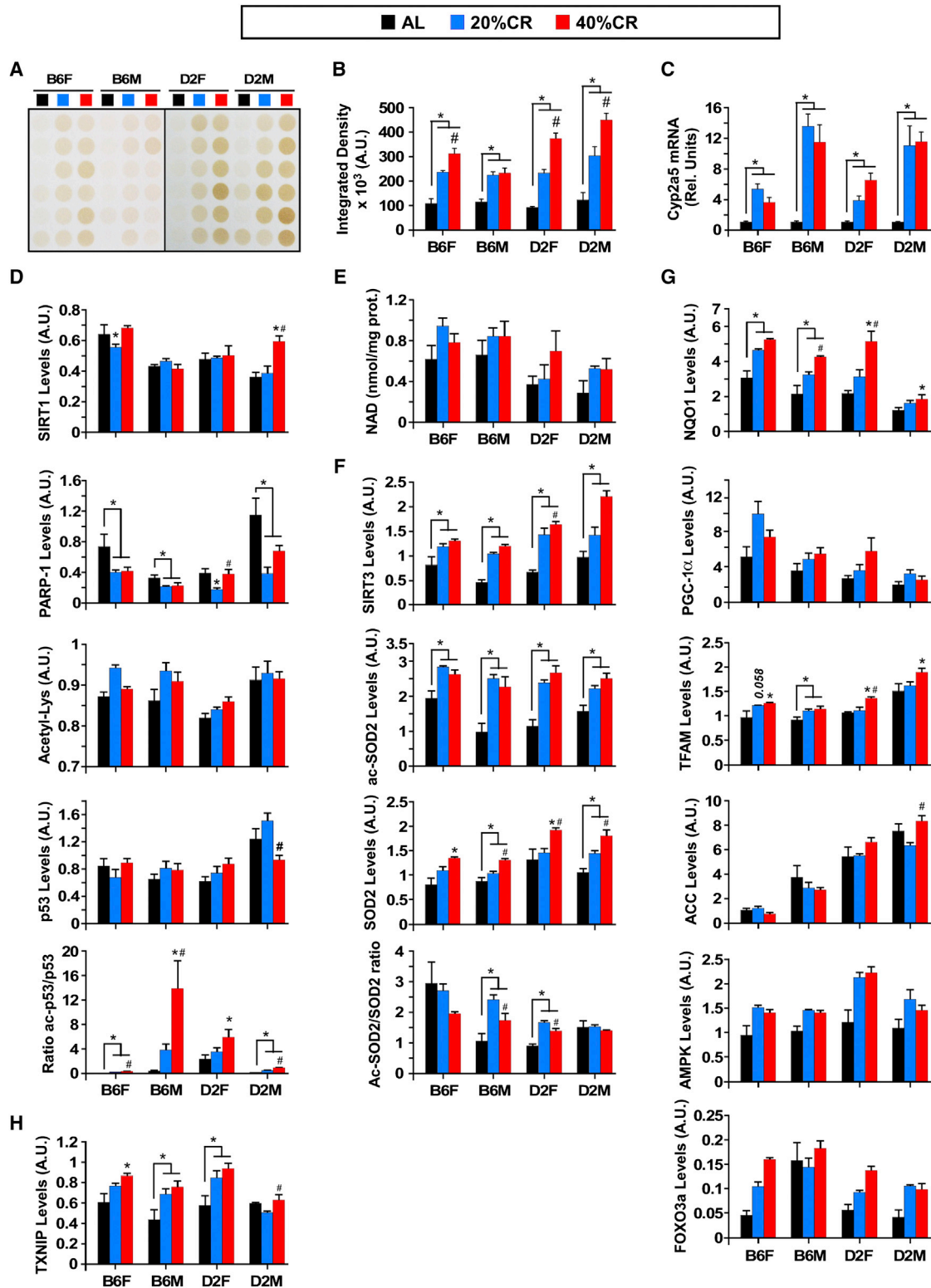


Figure 4. Effect of CR on Hydrogen Sulfide Production and Expression of Various Metabolically Relevant Protein Markers in Different Mouse Strains

(A) Production of H₂S in total liver lysates of AL- and CR-fed mice.
 (B) Densitometric quantification of H₂S production.
 (C) *Cyp2a5* mRNA levels measured by quantitative RT-PCR.

(legend continued on next page)

degradation through the proteasome, whereas D2 females utilize mostly aggregation. We next analyzed both the chymotrypsin-like (CTL) and peptidyl-glutamyl peptide-hydrolytic (PGPH or caspase-like) proteolytic activities of the proteasome in liver homogenates *in vitro* and differentiated between 26S and 20S by supplementing or not supplementing the reaction with ATP. Contrary to our prediction of CR-enhanced proteasome degradation in males, these studies revealed significant reduction of proteasome activity in all groups in response to CR (Figures 5C and 5D). This CR-induced inhibition of the proteasome activities was overall more pronounced in D2 females, especially in agreement with their higher content of both soluble and aggregate ubiquitinated proteins. When proteasomal activity was measured in the absence of ATP, most of the CR-induced alterations in chymotrypsin-like and caspase-like values were eliminated, suggesting less effect of CR on 20S proteasome activities (Figures S4A and S4B). A control experiment illustrated that preincubation of the liver homogenates with the potent proteasome inhibitor MG115 markedly suppressed protease activities measured in the absence or presence of ATP (Figure S4C).

Since the CR-induced reduction in polyubiquitinated proteins could not be attributed to enhanced proteasome activity, we next explored possible changes in autophagic pathways. CR has been shown to prevent the age-dependent decline in macroautophagy activity in rodent liver (Bergamini et al., 2003) and to upregulate autophagy-related genes and proteins in human skeletal muscle (Yang et al., 2016). Ubiquitinated proteins are amenable to degradation via macroautophagy, and blockage of this pathway leads to intracellular accumulation of K48- and K63-positive aggregates (Hara et al., 2006; Olzmann and Chin, 2008; Tan et al., 2008). Analysis of steady-state levels of LC3-II, the most commonly used marker to measure autophagic compartments (Kabeya et al., 2000), revealed that 40% CR significantly increased levels of LC3-II in B6 mice when compared to 20% CR (Figures 5E and 5F). A trend toward increased levels of LC3-II in D2 mice on CR was also noticeable, although it did not reach statistical significance. Increased levels of LC3-II could be indicative of increased autophagy induction or reduced autophagic flux (autophagosome/lysosome fusion). We next attempted to measure *ex vivo* rates of autophagic flux by changes in levels of LC3-II upon incubation of liver explants with protease inhibitors (Figures 5E and 5G). CR did not modify rates of LC3-II turnover, except for D2 females on 20% CR, which displayed significant reduction in LC3-II flux (Figures 5E and 5G). These findings suggest that the CR-induced increase in LC3-II levels was not a consequence of blockage of autophagosome clearance but rather was due to autophagy induction. To further test this possibility, we analyzed the autophagic compartments in transmission electron microscopy (TEM) images of

livers from mice on varying degrees of CR (Figures S4D–S4M). In agreement with the steady-state levels of LC3-II (Figure 5F), morphometric analysis revealed an expansion in number and size of autophagic vacuoles in animals subjected to CR. This increase was, however, more noticeable in the B6 females and D2 males (Figures S4D–S4G and S4I–S4L). Scoring of autophagic vacuoles as autophagosomes or autolysosomes (mature autophagosomes), using standard morphological criteria, revealed that the CR-induced expansion of the autophagic compartments in B6 females and D2 males was a result of increased numbers of both autophagosomes and lysosomes, in further support that CR induced autophagy in these groups (Figures S4F and S4K). Interestingly, all CR livers displayed a significant increase in lipid droplets with morphological signatures of lipophagy (Singh et al., 2009), which was rarely observed in the AL groups (Figures S4H and S4M). D2 males on CR had the highest frequency of lipophagy despite autophagic rates being comparable to those in CR-fed B6 females, which suggests possible differences in the type of autophagic cargo favored by each group.

To complete our analysis of the autophagic system, we also analyzed the effect of CR on hepatic chaperone-mediated autophagy, which has been shown to contribute to metabolic regulation *in vivo* (Schneider et al., 2014) and restore chaperone-mediated autophagy reverse aging phenotypes in liver (Zhang and Cuervo, 2008). The subpopulation of lysosomes normally active for chaperone-mediated autophagy (CMA) (those that contain the hsc70 chaperone in their lumen; Cuervo et al., 1997) was isolated from the livers of each of the groups, and their chaperone-mediated autophagy activity was compared using a well-established *in vitro* system. We did not find differences among the different groups in the ability of chaperone-mediated autophagy-active lysosomes to take up and degrade a pool of radiolabeled chaperone-mediated autophagy substrates (Figure 5H). In agreement with these findings, the levels of the two limiting chaperone-mediated autophagy lysosomal components, LAMP-2A (the CMA receptor) and lysosomal hsc70, remained unchanged upon CR in CMA-active lysosomes (Figures 5I and 5J, Figure S5). Interestingly, analysis of the same proteins in lysosomes with usual low CMA activity (CMA–) revealed that CR significantly increased levels of hsc70 in this group of lysosomes in the B6 males (Figure 5I) but not in the other groups of mice (Figure 5J, Figure S5). We confirmed using the *in vitro* assay that the higher abundance of hsc70 in the CMA– lysosomes from B6 males, when subjected to CR, increased their ability to perform CMA (Figure 5K shows proteolysis in intact lysosomes that recapitulates binding/uptake and degradation of proteins). Overall, these studies illustrate strain and sex differences in the effect of CR on the different proteolytic systems in the liver. Upregulation of different autophagy pathways by CR may

(D) Total liver lysates were immunoblotted with the indicated primary antibodies (see Figure S3B for full immunoblot images). Densitometric measurements of SIRT1, PARP-1, cellular acetylated proteins, total p53, and ratio of acetylated/total forms of p53 are depicted.

(E and F) NAD determination in liver lysates (E) and densitometric measurements of SIRT3, acetylated and total SOD2, and the ratio of acetylated/total forms of SOD2 (F). Full immunoblot images are depicted in Figure S4C.

(G) Densitometric measurements of NQO1, PGC-1 α , TFAM, ACC, AMPK, and FOXO3a are depicted. Full immunoblot images are shown in Figure S3D.

(H) Densitometric measurements of TXNIP (full immunoblot images in Figure S3D).

For (D, F, and H), immunoblot membranes were stained with Ponceau S (representative staining in Figure S3E), and each band was normalized to the total densitometric value of the Ponceau staining for that line. All data are the mean \pm SEM of six biological replicates per experimental group, 23–24 months of age, 17–18 months on diet. * $p < 0.05$ compared to AL; # $p < 0.05$ compared to 20% CR.

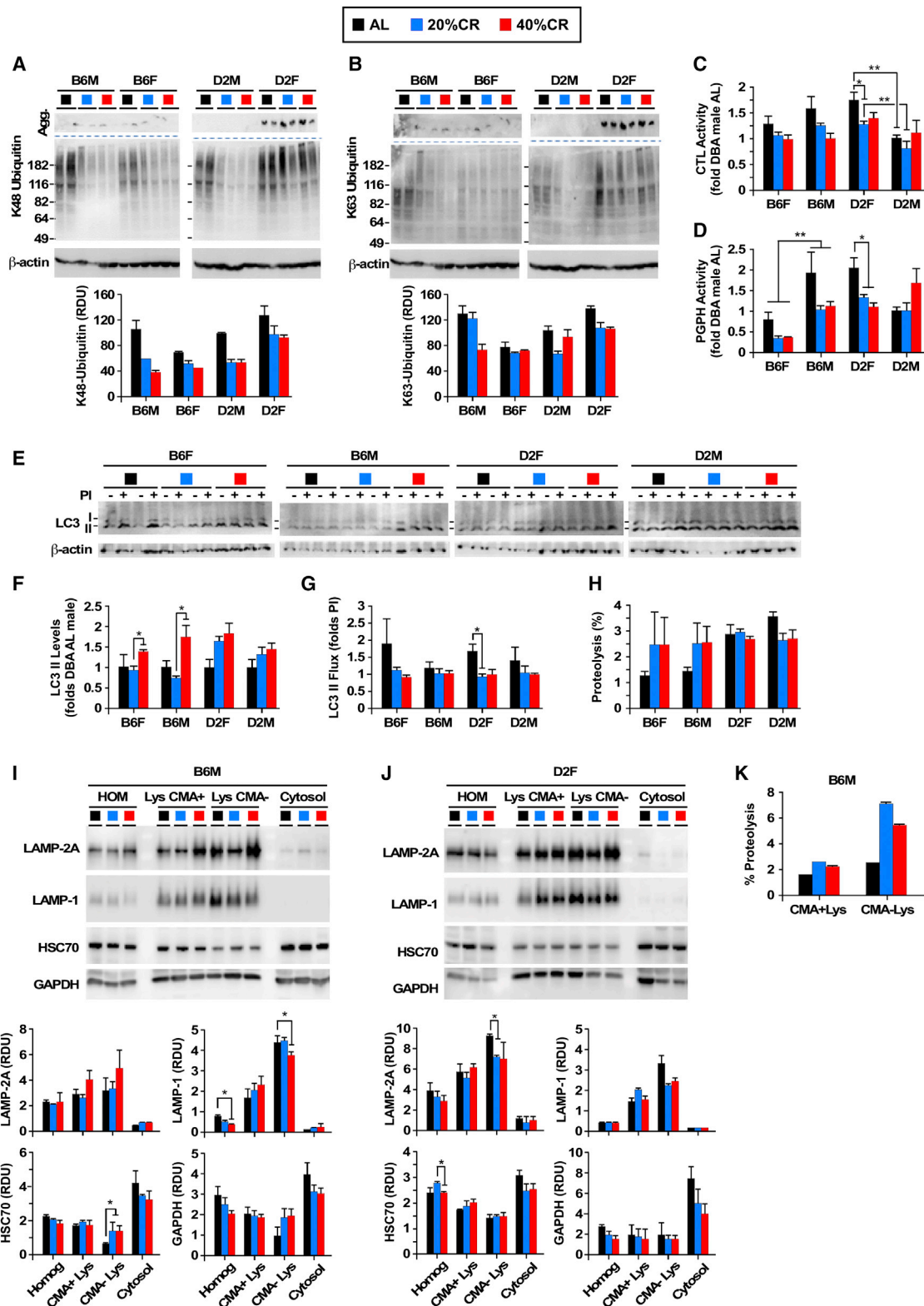


Figure 5. Changes in Proteostasis and Autophagy in Response to CR in Different Mouse Strains

(A and B) Immunoblot for K48- (A) and K63-linked (B) ubiquitinated proteins from liver homogenates. Bottom: densitometric quantification after actin normalization. n = 2.

(legend continued on next page)

contribute not only to the maintenance of protein homeostasis but also to improvements in hepatic carbohydrate and lipid metabolism directly through lipophagy (Singh et al., 2009) or through selective degradation of metabolic enzymes via chaperone-mediated autophagy (Schneider et al., 2014), which have a positive impact on the overall energetic balance of the organism.

Functional Mitochondria Are Required for the Life Extension Benefits of CR

The signature of transcripts that encode key enzymes implicated in the energy metabolism pathway was found to be rather complex in response to CR, with *Fh1* (mitochondrial fumarate hydratase) levels significantly increased in B6 and D2 females, but not males, whereas expression of *Pkm* (pyruvate kinase muscle isozyme) transcript was reduced only in CR-fed B6 male and female mice (data not shown). Quantitative RT-PCR analysis showed the significant increase in *Fh1* mRNA levels in B6 and D2 females on CR (Figure 6A) and selective reduction in *Mdh2* (mitochondrial malate dehydrogenase 2) expression in B6 females on 40% CR (Figure 6B). *Mdh2* affects the malate-aspartate shuttle and increases cellular antioxidant function. However, western blot analyses and in vitro enzymatic activity performed with liver lysates demonstrated that the total amount of MDH2 and its associated activity were significantly increased in all CR-fed groups of mice (Figures 6C and 6D), perhaps suggesting upregulation of TCA cycle activity, consistent with the metabolomics data.

The role of select enzymes implicated in mitochondrial respiration was then examined for their life-enhancing benefits in lower organisms. Based on our array and validation data, we selected *Fh1* and *Mdh2* because they were differentially altered in B6 females. When maintained in the absence of food or fed with standard laboratory diet (Figure S6A), *fem-1* (*hc17*) and Cy303 strains of *C. elegans* harboring genetic deletion (RNAi feeding) in *fum-1* (worm homolog of *Fh1*), *glna-2* (worm homolog of glutaminase 2), or *mdh2* lived significantly shorter than wild-type individuals, as evidenced by their reduced mean and median lifespan (Figures 6E–6G). Moreover, the absence of a mitochondrial genome in rho0 yeast cells severely reduced lifespan when fed either AL or CR diet and was accompanied by a significantly higher proportion of PI-positive yeast cells among rho0 cells compared to wild-type cells (Figure 6H). We further tested whether survival required *FUM1* and *MDH2*, the yeast homolog of *Fh1* and *Mdh2*. Deletion of *FUM1* rendered the cells unresponsive to the prolongevity effects of CR observed in wild-type yeast cells (Figure 6I). The impact of $\Delta mdh2$ was generally

milder with some lifespan extension in response to CR (Figure 6J). These results confirmed the essential requirement of functional mitochondria in the life-extending properties of CR. To further elucidate the potential role of the mitochondria in the unexpected response of B6 female mice to 40% CR, we produced cohorts of B6D2F1 and D2B6F1 offspring and placed them on 40% CR. Currently, with 25% of the cohorts dead, and based on an interim analysis of survival, there is a significant difference between the two F1 hybrid strains, whereby mice that inherited the B6 mitochondrial pool have a clearly diminished response to 40% CR (Figure 6K). Thus, the mitochondria function and haplotype play an essential role in the ability of model organisms to maximally reap the survival effects of CR.

To further assess the impact of CR on mitochondria, TEM of livers was carried out, and representative images are shown in Figure 6L. From these images, we obtained both planimetry and stereological data to characterize morphology of liver mitochondria in the experimental groups. There were significant changes in mitochondrial size depending on sex and strain. Remarkably, an increase of mitochondrial size was found in B6 and D2 males and in B6 females fed a 40% CR diet, but no increase was observed in D2 females fed the same diet (Figure S6B). With respect to 20% CR, mitochondrial size showed no or only a minor change in males from both strains, while unique patterns were observed in females, with a decrease in B6 and an increase in D2 mice. In contrast, the effect of CR on mitochondrial circularity was consistent in all experimental groups, with a marked decrease of circularity in 20% CR and a further decrease by 40% CR (Figure S6B), suggesting either increased mitochondrial biogenesis or possibly increased mitochondrial fusion. Stereological analysis was performed to obtain cell volume density (Vv), representing the cell volume fraction occupied by mitochondria per hepatocyte volume unit. For this parameter, the most consistent change was the increase by 40% CR in all groups regardless of strain or sex. In the case of 20% CR, we also observed a general trend toward an increase of Vv, although statistically significant differences were only found for B6 males and D2 females (Figure S6B). Since the increase of nuclear size is a well-established marker of aging in liver (Gregg et al., 2012), we also measured this parameter to assess if the observed structural changes in mitochondria were related to the improvement of liver preservation. Of note, the effects of dietary interventions on hepatocyte nuclear size paralleled those on mitochondrial circularity and roughly mirrored the changes in Vv, since a decrease of nuclear size was observed to occur in all groups, both with 20% and 40% CR, this latter intervention producing a more pronounced effect (Figure S6B).

(C and D) Chymotrypsin-like (CTL) (C) and peptidyl-glutamyl peptide-hydrolytic (PGPH) (D) proteasome activity measured in the presence of ATP in liver homogenates. Values are expressed relative to AL-fed D2 males, which were given an arbitrary value of 1. n = 3, 23–24 months of age, 17–18 months on diet. Values are mean \pm SEM. *p < 0.05, **p < 0.01.

(E) LC3-II levels and LC3-II flux measured by immunoblotting for LC3 in liver explants incubated or not with lysosomal protease inhibitors (PI, NH₄Cl, and leupeptin).

(F and G) Graphs show densitometric quantification of LC3 levels (F) and LC3 II flux (G). n = 4, 23–24 months of age, 17–18 months on diet.

(H) CMA activity as measured by percentage of proteolysis of radiolabeled pool of cytosolic proteins in isolated intact CMA+ lysosomes. n = 2, 23–24 months of age, 17–18 months on diet.

(I and J) Immunoblot for the indicated proteins in homogenate (HOM), CMA+ and CMA– lysosomes, and cytosol isolated from livers of B6 males (I) and (J) D2 females. Graphs (bottom) show densitometric quantification of LAMP-2A, LAMP-1, HSC70, and GAPDH.

(K) CMA activity as measured as in (I) in CMA+ (n = 2) and CMA– lysosomes isolated from B6 male mice (n = 3–4). Values are mean \pm SEM, 23–24 months of age, 17–18 months on diet. *p < 0.05, **p < 0.01, ***p < 0.001.

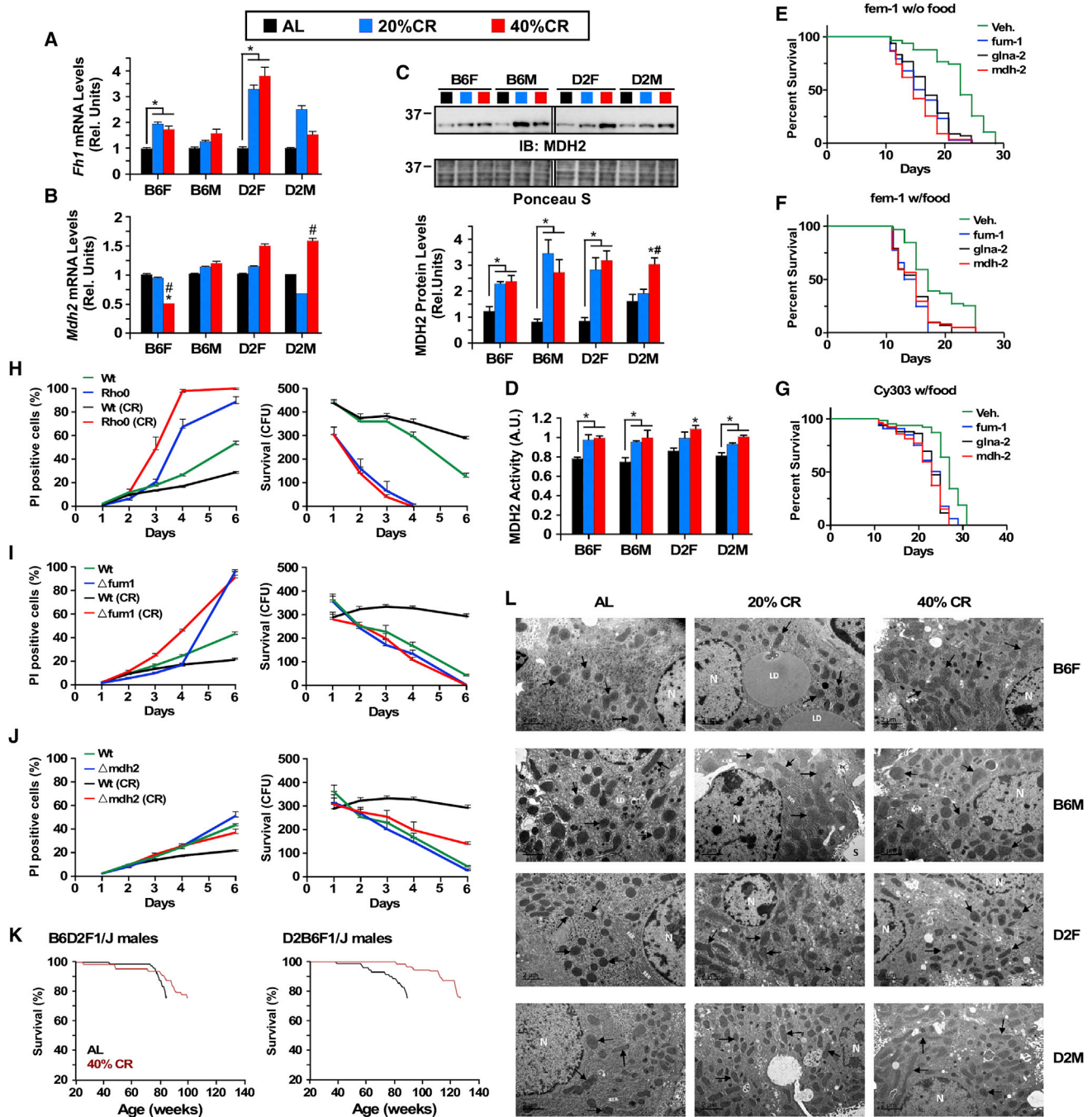


Figure 6. Functional Mitochondria Are Required for the Lifespan Extension Effects of CR

(A and B) *Fh1* (A) and *Mdh2* (B) mRNA levels were measured by quantitative RT-PCR. Bars represent mean \pm SEM of 4–6 biological replicates, 23–24 months of age, 17–18 months on diet. **p* < 0.05 compared to AL; #*p* < 0.05 compared to 20% CR.

(C and D) Mdh2 protein levels (C) and activity (D) in total liver lysates.

(E–G) Survival curves of *fem-1* (E and F) and *Cy303* strains (G) of *C. elegans* harboring genetic deletion in *fum-1*, *glna-2*, or *mdh-2*.

(H–J) Survival curves (right panels) and percent of PI-stained cells (left panels) of *rho0* (H), Δ *fum1* (I), and Δ *mdh2* (J) yeast cell mutants fed either AL or CR diet.

(K) Kaplan-Meier survival curves for B6D2F1/J and D2B6F1/J male mice either fed a standard diet AL or maintained on 40% CR. *n* = 60–75 mice per experimental group.

(L) Representative transmission electron microscopy images of liver sections of all 12 experimental groups, *n* = 4–6 biological replicates per experimental group, 23–24 months of age, 17–18 months on diet.

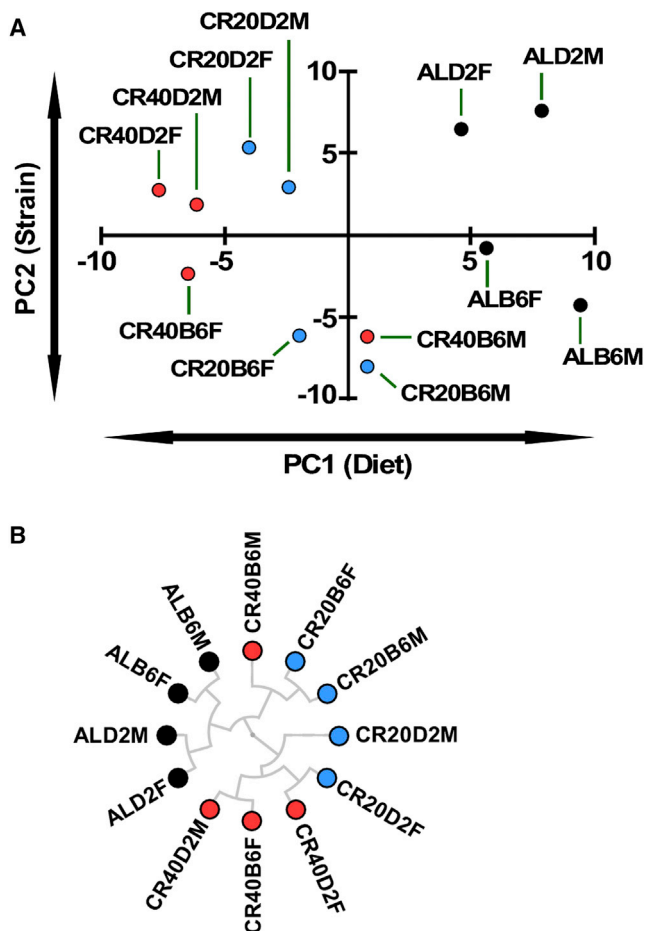


Figure 7. Interpretation of Various Data Sets that Include Phenotypic, Physiological, Biochemical, and Metabolomics Markers

(A and B) Principal component analysis (A) and hierarchical clustering (B) of the various experimental groups based on Z score-normalized behavioral, physiological, biochemical, and metabolomics data using uncentered similarity metrics and average linkage (see Figure S7 for a clustering of the input data).

No discernible differences in citrate synthase activity were observed except for a reduction in female B6 and D2 mice on 40% CR compared to AL controls (Figure S6C). Blue native electrophoresis was used to separate intact mitochondrial electron transport chain complexes in liver extracts, and the results indicated a significant increase in the levels of respiratory chain complexes I, II, and III in CR-fed D2 females, whereas B6 males and females on 40% CR showed higher complex I and II levels, respectively (Figures S6D and S6E). Optimal activity of complex I requires the interaction with prohibitin (Phb), a major mitochondrial inner membrane protein implicated in cristae morphogenesis and functional integrity of mitochondria (Artal-Sanz and Tavernarakis, 2009; Merkwirth et al., 2008). A significant reduction in Phb levels was observed in B6 and D2 males in response to CR, which was in sharp contrast to the 3- to 4.5-fold increase in the amount of Phb protein in CR-fed D2 females (Figures S6F and S6G). This event did not occur in B6 females on CR. Strikingly, the expression of the classical mitochondrial cochaperone Hsp60 was severely abrogated in B6 and D2 females, but not

males (Figures S6F and S6G). These results indicate sex-specific differences in the metabolic regulation of mitochondrial architecture and function, which likely results in distinct variation in healthy aging and lifespan extension.

Global Hierarchical Clustering

To further analyze the extensive amount of data presented here and to obtain a global unbiased understanding of which factors might contribute to longevity, we performed PCA of Z score-normalized behavioral, physiological, and biochemical data (Figure 7A, Figure S7). Notably, the strongest principal component (PC1) appeared to be the dietary intervention, while PC2 appeared to describe changes associated with strains supporting the notion of a universal response to dietary interventions across B6 and D2 mice. We further performed hierarchical clustering (Figure 7B) of this data, which revealed good separation between AL-fed groups and the CR groups and, interestingly, seemed to facilitate association between the groups that had the greatest benefit of lifespan (CR20B6F, CR20B6M, and CR40B6M) and those that had less benefit (CR40B6F, CR20D2F, CR40D2F, CR20D2M, and CR40D2M) (Figure 7B). Notably, by performing the same analysis on the input data, the closest association to maximum lifespan was fat mass, while NAD⁺ levels appeared to correlate the strongest with mean lifespan (Figure S7). These data support the findings that maintenance of mitochondrial function, NAD⁺ levels, and preservation of essential fat mass with age are important predictors of lifespan.

DISCUSSION

CR has long been the measuring stick and gold standard for alternative strategies to improve health and survival in biomedicine by manipulating cellular and molecular mechanisms of aging. However, emerging evidence calls into question the universality of the effects of CR in extending mean and maximal lifespan. These life extension effects may be influenced by common experimental variables such as species, genetic background, sex, macronutrient composition and meal timing, degree of restriction, age of onset, and their interactions. In this study, we have systematically addressed the effects on health and survival of three factors—genetic background, sex, and degree of CR—and examined key physiological hallmarks of the CR response (body weight, core body temperature, insulin sensitivity, metabolism, pathology, and survival) to determine if there is an optimal level of CR that will maximize health and survival in two strains of mice for both sexes. Our results provide further evidence that multiple factors alter the response to CR and that while the effect of CR on health appeared consistent across strains and sexes, survival was not correlated with CR in all cases.

The universal effects of CR on lifespan were challenged recently in a number of studies in wild-derived mice (Harper et al., 2006), inbred strains (Fernandes et al., 1976; Forster et al., 2003; Goodrick et al., 1990; Harrison and Archer, 1987; Turturro et al., 2002), and recombinant inbred strains (Liao et al., 2010; Rikke et al., 2010). Indeed, body weight loss and reduction in core body temperature were not proportional to the number of calories consumed or to survival. Mice on CR weighed less than AL-fed controls, although this is not always

proportional to their level of restriction. Mice that responded the best on survival outcomes were those that preserved their fat mass better into the second year of life, suggesting that there is a minimum level of adiposity that is necessary for the full benefit of CR and that the contribution of this organ to metabolic regulation under CR condition is crucial. These results are congruent with the work of [Liao et al. \(2011\)](#) showing that strains of mice with the lowest reduction in fat under CR were more likely to have extended lifespan. Furthermore, long-lived strains, such as the Ames and Snell dwarf mice, have higher percentages of body fat even though they are smaller than their littermates. Indeed, recent work has shown in humans that slight overweight is associated with the lowest level of all-cause mortality ([Flegal et al., 2013](#); [Grabowski and Ellis, 2001](#)).

The recognition that fat tissue is an endocrine organ capable of producing adipokines led us to measure the circulating levels of leptin and adiponectin, two regulators of long-term energy balance ([Mitchell et al., 2015b](#)). Serum leptin was lower but adiponectin was higher in CR-fed mice compared to their AL-fed controls, which can be attributed to the reduction in body weight and potential reprogramming of hepatic fat metabolism in response to CR ([Kuhla et al., 2014](#)). CR in rodents is also known to reduce fertility, perhaps as an evolutionary response to hunger, enabling the shutdown of reproduction and the investment of all energy into repair mechanisms and survival ([Kirkwood, 2002](#); [Kirkwood and Shanley, 2005](#)). Here, we showed a dramatic reduction in expression of liver MUPs, which are linked to maintenance of organ size and male sexual signaling. These changes in MUPs were mostly closely linked to organ size and leptin levels. In accordance, hepatocyte nuclear size, which is known to increase with aging, possibly due to enhanced polyploidy ([Gregg et al., 2012](#)), was significantly lower in all CR groups compared with their AL counterparts, regardless of sex and strain, indicating a better preservation of liver homeostasis by CR.

The reduction in body temperature (T_b) has been postulated to play a role in the CR-promoting effects on lifespan in rodents and non-human primates ([Duffy et al., 1989](#); [Lane et al., 1995](#); [Mitchell et al., 2015a](#); [Speakman and Mitchell, 2011](#); [Turturro and Hart, 1991](#)). Interestingly, strains of mice that maintain high T_b are more likely to have extended lifespan under CR ([Speakman and Mitchell, 2011](#)). While this is contradictory to the suggestion that lowered T_b is a contributing factor to lifespan extension under CR ([Speakman and Mitchell, 2011](#)), it certainly highlights that there is more complexity to the CR phenomenon, especially when performing comparisons across mouse strain and sex. Our findings are in concordance with previous studies, with the exception of B6 female mice on CR. In these mice, T_b was significantly higher with 20% CR than in B6 females on AL or 40% CR. Alteration in heat production or heat loss and change in metabolic rate and/or activity could account for the increased T_b in B6 female mice on 20% CR. The preservation of fat mass means more insulation and lower rate of health decline as these mice age, which may have contributed in having opposing effects on the classical T_b response to CR ([Rikke and Johnson, 2007](#)). Even though metabolic rate and activity level were not measured, it is believed that lower T_b contributes to longevity through a direct effect on reducing pathologies ([Speakman and Mitchell, 2011](#)). As demonstrated in all experimental groups,

with the exception of D2 males, CR feeding induced a reduction in both the number and age of onset of pathologies.

Improvement in insulin sensitivity and signaling via the insulin/IGF-1 signaling pathway is a proposed mechanism through which CR retards aging and promotes lifespan ([Milman et al., 2014](#)). Genetic mutations in growth hormone, IGF-1 receptor, or downstream effectors of insulin/IGF-1 signaling (i.e., PI-3 kinase and FOXO) have been associated with increased lifespan ([Flurkey et al., 2001, 2002](#); [Hsieh et al., 2002](#); [Shimokawa et al., 2015](#); [Sun et al., 2013](#)). Data from a study using recombinant inbred strains showed that plasma IGF-1 levels were inversely correlated with median lifespan ([Yuan et al., 2009](#)). Further, we have recently shown that high IGF-1 is correlated with increased risk of cancer, and men with low IGF-1 because of GHR deficiency are fully protected against cancer ([Guevara-Aguirre et al., 2011](#)). Here, fasting levels of insulin, glucose, and IGF-1 were reduced with CR across all experimental groups, thus representing a global and consistent effect of CR on improving insulin sensitivity ([Mitchell et al., 2015b](#)). In most cases 20% CR was sufficient to produce a dramatic decrease in these parameters with little to no further benefit by 40% CR. The reduction in age-associated pancreatic islet hypertrophy combined with enhanced insulin sensitivity and lower insulin levels is likely to represent an important—although almost certainly not exclusive—mechanism by which CR increases longevity ([Masternak et al., 2009](#)). Although the levels of IGF-1 did not correspond to extended longevity in CR-fed mice, the possibility exists that higher IGF-1 helps improve health, while lower IGF-1 levels are associated with increased lifespan in response to CR. In this study, the shortest-lived animals (B6 females on 40% CR and all CR-fed D2 mice) had very low circulating levels of IGF-1 combined with high circulating IGF-1 levels. Indeed, low levels of IGF-1 and muscle mass have been shown to be negatively correlated with decreases in median and maximal lifespan in mice ([Sharples et al., 2015](#); [Yuan et al., 2009](#)).

The integration of physiological outcomes and hepatic transcriptomic and metabolomics data have provided the necessary tools to further examine the contribution of mouse strain and sex and the level of CR toward the lifespan trajectories. The overall buildup of metabolites indicates that the liver of CR-treated mice functions mainly in catabolic mode within mitochondria, with fatty acid β -oxidation catabolically driving the TCA cycle. In addition, a profile consistent with anaplerotic replenishment via amino acids (both ketogenic and gluconeogenic) and the urea cycle via fumarate could be observed. Under these conditions, the anaplerotic filling of the TCA cycle together with the energetic fatty acid fueling of mitochondria render a metabolism relying less on glucose. The apparent depression of intermediate levels of glycolytic, pentose phosphate, and glycogen pathways and the increased insulin sensitivity (e.g., significantly lower HOMA-IR index) exhibited by the CR-treated mice support this notion. In response to CR, liver metabolite profiles showed an enhancement in mitochondrial respiration driven by fatty acid degradation, which was accompanied by increased expression of respiratory complexes and which is expected from greater use of fat as fuel source ([Bruss et al., 2010](#)) and concomitant alteration in body fat composition.

Consistent with the current literature, our transcriptomic analysis indicated a strong impact of CR on pathways implicated in

proteostasis, energy metabolism, and mitochondrial bioenergetics. Loss of proteostasis is a common hallmark of aging that has been shown to be prevented by CR (Kaushik and Cuervo, 2015), although with some sex differences, we found reduced levels of polyubiquitinated proteins with CR that cannot be attributed to enhanced proteasome activity, since the activities of this major cellular protease were instead lower in CR mice. It is possible that reduced overall protein synthesis/ubiquitination contributes to their lower abundance in CR, but we propose that, at least in some species and sex, increased autophagy could be behind the CR-induced proteostasis changes. Beyond its role in protein homeostasis, autophagy has been proven essential for specific adaptation to nutritional availability, during both nutrient excess and scarcity (Madrigal-Matute and Cuervo, 2016). Interestingly, TXNIP has also a role in stress-induced macroautophagy (Qiao et al., 2015), one of the hallmarks of aging. Although CR increased overall autophagic activity in most of the experimental groups, we found marked sex and strain differences in the intensity of this autophagic response and the type of autophagy preferentially induced. Both macroautophagy and chaperone-mediated autophagy contribute to regulate hepatic metabolism but through different mechanisms (Madrigal-Matute and Cuervo, 2016). Macroautophagy directly mobilizes energy stores, such as lipid droplets, and also regulates metabolic flux by controlling mitochondria abundance through mitophagy. Whereas all CR groups showed reduced mitochondria circularity, suggestive of reduced mitophagy, only some of them displayed enhanced lipophagy (Gomes et al., 2011; Twig et al., 2008). It is possible that changes in lipid metabolism are a consequence of the observed increase in chaperone-mediated autophagy activity, which was recently shown to contribute to regulation of hepatic lipid metabolism through the degradation of key enzymes in these pathways (Kaushik and Cuervo, 2015; Schneider et al., 2014). Taken together, our results indicate that the increased bioavailability of amino acids and fatty acids in the liver of CR-fed mice may be derived from activation of autophagic pathways. This metabolic switch could account for the increase in health span and lifespan observed in most CR-fed animals.

In mouse hepatocytes we have shown that aging induces a decrease in mitochondrial mass together with reduction in individual mitochondria size and changes in the expression pattern of proteins related to fusion/fission dynamics (Khraiwesh et al., 2013, 2014; López-Lluch et al., 2006). However, 40% CR alleviated most of these effects by inducing increases in individual mitochondria size and volume fraction occupied by mitochondria. The conclusion was reached that CR results in a higher number of more efficient mitochondria. The results reported here show a general increase in mitochondrial mass (expressed as volume density) with CR regardless of sex or strain of mice, although 40% CR appears to have a more pronounced effect on this parameter. In addition, mean mitochondrial size varied depending on the strain, sex, and the degree of CR, but with the exception of D2 females, 40% CR induced an increase in mitochondrial area, which fit well with the results reported by Khraiwesh et al. (2014) in B6 mice. Moreover, CR was found to uniformly decrease circularity in mitochondria in all of the dietary groups. It has been shown that mitochondrial shape is closely related to mitophagy in such a way that elongated mitochondria

are preserved from mitophagy (Gomes et al., 2011). Therefore, the possibility exists that selective mitophagy (depending on the mitochondrial haplotype) accounts for the preservation of efficient mitochondria in CR-fed animals.

In *C. elegans*, it has been clearly demonstrated that aging induces a decline in mitochondrial function that leads to the activation of specific pathways (Chang et al., 2015) and an increase in reactive oxygen species (ROS). Orthologs of p53 and NRF2 (CEP-1 and Skin1) are among other important mediators of longevity induced by mild mitochondrial dysfunction in the worm. SKN-1 directly associates with the mitochondria and has been shown to be critical to the response to CR. Moreover, we have shown that Nrf2 is essential for the anti-carcinogenic effects of CR in mice (Pearson et al., 2008b). Based on our transcriptomic analysis, we genetically manipulated a selection of these transcripts in yeast and worms to demonstrate that the maintenance of healthy and functional mitochondrial population is necessary for the pro-survival effects of CR in these two organisms. Furthermore, two F1 hybrid strains produced from the cross of B6 and D2 mice responded to 40% CR in a maternally inherited manner, suggesting the importance of the inherited mitochondria pool for the responsiveness to this dietary intervention.

Even if long-term CR was shown to benefit human aging, confer cancer protection, and increase longevity, it would be extremely difficult to achieve adherence to such a stringent diet that might require a reduction of 20%–40% in daily caloric intake. Human CR studies have shown clear effects on metabolic and molecular health in humans, including reduced multiple risk factors implicated in the pathogenesis of type 2 diabetes, obesity, cardiovascular disease, cancer, stroke, vascular dementia, and liver and kidney diseases (Fontana et al., 2014; Longo et al., 2015). More research is needed to fine-tune our understating of the pathways implicated and how to precisely modulate them, but the evidence of the protective effects of CR in humans is clear and powerful. To this end, considerable investment has been focused on dissecting the pathways that regulate the beneficial effects of CR to spur development of pharmacological agents potentially acting as CR mimetics. In recent years, dietary regimens, CR mimetics, and small molecules have generated promising results in anti-aging trials. Not surprisingly, most of these interventions have strain-, diet-, and sex-specific effects on health and survival in mice (Anisimov et al., 2008; Harrison et al., 2009, 2014; Martin-Montalvo et al., 2013; Miller et al., 2011, 2014; Pearson et al., 2008a; Strong et al., 2008, 2013). Nonetheless, these molecules are bolstering our understanding about their molecular mechanisms and their use for aging and age-related chronic diseases such as cancer, cardiovascular disease, and neurodegenerative disorders. A logical extension of these interventions is aimed at understanding the proper context in which the application of these interventions will be most beneficial to humans, and to identify which biomarkers are associated with the best predictors of health span and lifespan. These biomarkers could be part of the standard screening protocol to identify earlier and more effective interventions and treatments in the clinic than the current standard of 3+ years in a mouse longevity study. It is through the innovative and unique interdisciplinary approach of geroscience that we will gain further understanding of the biological

mechanisms underlying aging and age-related disease and disability. While great strides have been made by scientists engaged in aging research, the recent formation of the Trans-NIH GeroScience Interest Group, the Intervention Testing Program, and other similar groups have served as catalysts for major leaps in this field.

Conclusion

CR effects on survival are not universal. We have demonstrated a strain-, sex-, and dose-dependent effect of CR on health and survival in two strains of mice. It appears that the interaction and contribution of each of these factors may have an impact on the overall energetic balance of the organism, which determines the outcome on health and survival. Our results provide evidence for the complex relationship between health and survival in mouse longevity studies and suggest that to attain the maximal benefits of CR, the maintenance of healthy and functional mitochondria and active autophagy that leads to improvements in carbohydrate and lipid metabolism is required to allow metabolic flexibility and preservation of a healthy amount of body fat into old age.

EXPERIMENTAL PROCEDURES

Animals and Diets

Male and female C57BL/6J and DBA2/J mice were obtained from the Jackson Laboratory and then bred in house at the National Institute on Aging (NIA) in order to obtain a sufficient number of mice per group. In an ongoing study, F1 offspring were bred in house at NIA to generate male B6D2F1/J and D2B6F1/J mice. Litters were maintained with approximately eight pups to minimize the potential confounding effect of a crowded litter (Sadagurski et al., 2014). Mice were housed in cages of 3–4 with ad libitum (AL) access to water at the Gerontology Research Center. Mice were fed house chow (2018 Teklad Global 18% Protein Rodent Diet, Harlan Teklad) either AL or at 20% or 40% CR starting at 6 months of age for the remainder of their lives. F1 offspring were fed AL and 40% CR, and none of the parents used to generate these specific F1 mice underwent CR. A gradual stepwise reduction in food intake by increments of 10% per week was carried out for CR mice. Body weight and food intake were monitored biweekly. CR mice were fed daily at 7:30 a.m. \pm 1 hr, and food was placed onto the floor of the cage. AL mice were fed in the hopper. Animal rooms were maintained at 20°C–22°C with 30%–70% relative humidity and a 12-hr light/dark cycle. In March 2013, all animals were moved to the new NIA Biomedical Research Center (across the road), and for the next 2 weeks, no change in food consumption, body weight, or unexpected increase in mortality of mice was recorded. For the longevity study, the following mice per group were used: n = 50 B6 female and male mice per experimental group, n = 63 D2 female AL, n = 58 D2 female 20% CR, n = 61 D2 female 40% CR, n = 60 D2 male AL, n = 59 D2 male 20% CR, n = 61 D2 male 40% CR. For the F1 study, there were n = 72 and n = 66 B6D2 male mice on AL and 40% CR diets, respectively, while there were n = 64 and n = 69 D2B6 male mice on AL and 40% CR diets, respectively. All animal protocols were approved by the Animal Care and Use Committee (405-LEG-2012, 405-TGB-2015, and 405-TGB-2019) of the National Institute on Aging.

Survival Study

Animals were inspected twice daily for health issues, and deaths were recorded for each animal. Moribund animals were euthanized, and every animal found dead or euthanized was necropsied. The criteria for euthanasia were based on an independent assessment by a veterinarian according to AAALAC guidelines, and only cases where the condition of the animal was considered incompatible with continued survival are represented as deaths in the curves. Animals removed at sacrifice were considered as censored deaths. Additional details are provided in the [Supplemental Information](#).

Sacrifice and Collection of Tissues

At 23–24 months of age (17–18 months of dietary intervention), six mice per diet group were sacrificed over 3 consecutive days from 7 a.m. to 11 a.m. Mice were euthanized by cervical dislocation and tissues were rapidly collected, weighed, and then snap frozen in liquid nitrogen or processed for further analyses as detailed below. A second cohort of animals (4–6 mice per group, age 17–23 months, diet 11–17 months) was anaesthetized with ketamine-xylazine, and then oxygenated Krebs-Henseleit buffer was briefly perfused through the liver vasculature at low pressure to wash blood out of the sinusoids. A portion of the liver was fixed for electron microscopy (EM), while the remainder was used for functional autophagy measurements as described below. All mice were sacrificed between 7 and 11 a.m. On the day of the sacrifice for both cohorts of animals, mice were on their normal feeding cycles, not fasted (mice on a CR diet were not fed their daily ration, while AL mice were allowed to eat AL until sacrifice).

Body Composition

Measurements of lean, fat, and fluid mass in live mice were acquired by nuclear magnetic resonance (NMR) using the Minispec LF90 (Bruker Optics).

Rectal Temperatures

Rectal temperature was measured in mice with a BAT-12 Microprobe Thermometer with a RET3 rectal probe for mice (Physitemp Instruments, Inc.). Additional details are provided in the [Supplemental Information](#).

HOMA Calculation

Insulin resistance was calculated from fasted glucose and insulin values using the HOMA2 Calculator software available from the Oxford Centre for Diabetes, Endocrinology and Metabolism, Diabetes Trials Unit website (<http://www.dtu.ox.ac.uk>).

Pancreatic Islet Tissue Processing, Immunohistochemistry, and Image Analysis

Paraffin-embedded pancreatic tissue was sectioned, immunostained for insulin and glucagon, and imaged. Quantification of the images was performed using the pancreatic islet analytical software program, Pancreas++. The [Supplemental Information](#) contains full methodological details.

Gene Expression

Microarray and quantitative RT-PCR techniques were carried out according to standard procedures to determine the effects of sex, gender, and degree of CR on gene expression in mouse liver. Full methodological details are described in [Supplemental Experimental Procedures](#).

Yeast CR Experiments and Lifespan Studies in Worms

Chronological aging experiments in wild-type yeast (*S. cerevisiae* BY4741) and respective mutant strains were performed in two types of media, defined as SCD and CR media.

Lifespan analysis was carried out in two stains of *C. elegans* supplied with vehicle RNAi or with specific RNAi supplementation as food source. Full methodological details for both invertebrate studies are described in [Supplemental Experimental Procedures](#).

Metabolomics

Metabolomics analysis on mouse liver extracts was performed by the UC Davis West Coast Metabolomics Center according to established procedures (see [Supplemental Information](#) for full methodological details).

Determination of NAD⁺ and Hydrogen Sulfide Levels

The measure of NAD⁺ and hydrogen sulfide was carried out in liver extracts according to well-established procedures. Full methodological details are described in the [Supplemental Information](#).

Tissue Processing for Planimetric and Stereological Analysis

The left lateral lobe of perfused liver was sectioned and fixed for EM to assess general structural preservation and quantification of hepatocyte nuclear area. Whole hepatocyte micrographs were taken for stereological analysis of mitochondrial abundance, and the mitochondrial size and shape were quantified

by planimetric analysis. Full methodological details can be found in the [Supplemental Information](#).

Gel Electrophoresis and Western Blotting

Separation of mouse liver extracts and mitochondrial preparations for the detection of specific proteins was carried out according to standard procedures as described in the [Supplemental Information](#).

Functional Measures of Autophagy

Mouse liver lysosomes were isolated from a light mitochondrial-lysosomal fraction in a discontinuous metrizamide density gradient, and a fraction enriched in the subpopulation of lysosomes active for chaperone-mediated autophagy was further separated. Full methodological details for proteolysis by intact lysosomes *in vitro*, LC3 flux, measurement of proteasome activity, and quantification of EM pictures are summarized in [Supplemental Information](#).

Hierarchical Clustering

Quantitative behavioral, physiological, biochemical, and metabolomics data were Z score normalized across the 12 experimental groups. Unsupervised hierarchical clustering was performed on the normalized data with a custom script using average linkage and uncentered similarity metrics.

Statistics

Data are presented as mean \pm SEM unless otherwise specified. Analyses were performed using Excel 2010 (Microsoft), IBM SPSS Statistics, or SigmaStat 3.0 (Aspire Software International). The survival analyses were implemented in R (The R Development Core Team) from scratch using the methodological references given. Comparisons between groups were performed using Student's t test or one-way ANOVA with post hoc tests as specified. Metabolite analysis from metabolomics data was performed using two-way ANOVA as a function of treatment and sex for each mouse strain with Tukey's post hoc analysis. A p value < 0.05 was considered statistically significant.

ACCESSION NUMBERS

Raw microarray datasets have been submitted to the NCBI GEO database under accession number GEO: GSE81959.

SUPPLEMENTAL INFORMATION

Supplemental Information includes Supplemental Experimental Procedures, seven figures, and six tables and can be found with this article online at <http://dx.doi.org/10.1016/j.cmet.2016.05.027>.

AUTHOR CONTRIBUTIONS

R.d.C., D.K.I., K.J.P., M.B., R.M.A., P.N., D.A.S., L.F., and D.L.L. conceived and designed the study; S.J.M., J.M.M., M.S.-K., M.G.-F., D.W., A.A., V.G., T.M.W., and H.H.P. performed most experiments; E.F. and V.B. conducted the worm studies while F.B., L.H. and F.M. carried out yeast lifespan studies; M.A. and S.C. ran the metabolomics studies; J.A.G.-R., M.C.-R., M.I.B., and J.M.V. liver transmission electron microscopy; J.M.M., S.K., B.P., and A.M.C., proteostasis network and associated TEM imaging; H.C., J.M.E., pancreatic islets work; D.W.F. and J.A.B., NAD analysis; C.H. and J.R.M., hydrogen sulfide analysis; J.D., T.M.B., and D.B.A., mouse lifespan analysis; J.W. and P.C., IGF-1 and IGF1R studies; Y.I. and G.H., histopathology; M.B., K.G.B., and Y.Z., microarray analysis; M.B., R.d.C., S.J.M., M.S.-K., M.A., S.C., F.M., J.M.V., and A.M.C. wrote the manuscript; and most authors contributed to the editing and proofreading of the final draft.

ACKNOWLEDGMENTS

This work was supported in part by the Intramural Research Program of the National Institute on Aging, NIH, and by NIH grants R01 AG043483 and R01 DK098656 (J.A.B.), NIH grant AG031782 (A.M.C.), and the Proteostasis of Aging Core AG038072 (A.M.C.). J.M.M. was supported by a postdoctoral fellowship from the American Diabetes Association, grant 1-15-MI-03. P.C.

was supported by NIH grants (1P01AG034906, 1R01GM090311, and 1R01ES 020812). F.M. is grateful to the FWF for grants LIPOTOX, I1000, P27893, P29203, and P24381-B20 and the BMWFW for grants "Unconventional Research" and "Flysleep" (80.109/0001-WFV/3b/2015). J.M.V. was supported by the Spanish Ministerio de Economía y Competitividad (grants BFU2011-23578 and BFU2015-64630-R). The authors thank the personnel from the Servicio Centralizado de Apoyo a la Investigación (SCAI; University of Córdoba) for technical support. Special thanks to the members of the Translational Gerontology Branch and the Comparative Medicine Section of the National Institute on Aging. In particular we acknowledge Paul Bastian, Elin Lehmann, Frances Fan, Robin Minor, Dawn Nines, and Dawn Boyer.

Received: May 19, 2016

Revised: May 27, 2016

Accepted: May 31, 2016

Published: June 14, 2016

REFERENCES

- Abu-Bakar, A., Lämsä, V., Arpiainen, S., Moore, M.R., Lang, M.A., and Hakkola, J. (2007). Regulation of CYP2A5 gene by the transcription factor nuclear factor (erythroid-derived 2)-like 2. *Drug Metab. Dispos.* **35**, 787–794.
- Adamovich, Y., Shlomai, A., Tsvetkov, P., Umansky, K.B., Reuven, N., Estall, J.L., Spiegelman, B.M., and Shaul, Y. (2013). The protein level of PGC-1 α , a key metabolic regulator, is controlled by NADH-NQO1. *Mol. Cell. Biol.* **33**, 2603–2613.
- Anisimov, V.N., Berstein, L.M., Egormin, P.A., Piskunova, T.S., Popovich, I.G., Zabezhinski, M.A., Tyndyk, M.L., Yurova, M.V., Kovalenko, I.G., Poroshina, T.E., and Semenchenko, A.V. (2008). Metformin slows down aging and extends life span of female SHR mice. *Cell Cycle* **7**, 2769–2773.
- Anson, R.M., Guo, Z., de Cabo, R., Iyuan, T., Rios, M., Hagepanos, A., Ingram, D.K., Lane, M.A., and Mattson, M.P. (2003). Intermittent fasting dissociates beneficial effects of dietary restriction on glucose metabolism and neuronal resistance to injury from calorie intake. *Proc. Natl. Acad. Sci. USA* **100**, 6216–6220.
- Artal-Sanz, M., and Tavernarakis, N. (2009). Prohibitin couples diapause signalling to mitochondrial metabolism during ageing in *C. elegans*. *Nature* **461**, 793–797.
- Bartke, A., Mastemak, M.M., Al-Regaiey, K.A., and Bonkowski, M.S. (2007). Effects of dietary restriction on the expression of insulin-signaling-related genes in long-lived mutant mice. *Interdiscip. Top. Gerontol.* **35**, 69–82.
- Barzilai, N., Banerjee, S., Hawkins, M., Chen, W., and Rossetti, L. (1998). Caloric restriction reverses hepatic insulin resistance in aging rats by decreasing visceral fat. *J. Clin. Invest.* **101**, 1353–1361.
- Berg, B.N., and Simms, H.S. (1960). Nutrition and longevity in the rat. II. Longevity and onset of disease with different levels of food intake. *J. Nutr.* **71**, 255–263.
- Bergamini, E., Cavallini, G., Donati, A., and Gori, Z. (2003). The anti-ageing effects of caloric restriction may involve stimulation of macroautophagy and lysosomal degradation, and can be intensified pharmacologically. *Biomed. Pharmacother.* **57**, 203–208.
- Breese, C.R., Ingram, R.L., and Sonntag, W.E. (1991). Influence of age and long-term dietary restriction on plasma insulin-like growth factor-1 (IGF-1), IGF-1 gene expression, and IGF-1 binding proteins. *J. Gerontol.* **46**, B180–B187.
- Bruss, M.D., Khambatta, C.F., Ruby, M.A., Aggarwal, I., and Hellerstein, M.K. (2010). Calorie restriction increases fatty acid synthesis and whole body fat oxidation rates. *Am. J. Physiol. Endocrinol. Metab.* **298**, E108–E116.
- Cantó, C., Menzies, K.J., and Auwerx, J. (2015). NAD(+) Metabolism and the Control of Energy Homeostasis: A Balancing Act between Mitochondria and the Nucleus. *Cell Metab.* **22**, 31–53.
- Chang, H.W., Shtessel, L., and Lee, S.S. (2015). Collaboration between mitochondria and the nucleus is key to long life in *Caenorhabditis elegans*. *Free Radic. Biol. Med.* **78**, 168–178.
- Chattopadhyay, M., Kodala, R., Nath, N., Street, C.R., Velázquez-Martínez, C.A., Boring, D., and Kashfi, K. (2012). Hydrogen sulfide-releasing aspirin

- modulates xenobiotic metabolizing enzymes in vitro and in vivo. *Biochem. Pharmacol.* **83**, 733–740.
- Cheney, K.E., Liu, R.K., Smith, G.S., Leung, R.E., Mickey, M.R., and Walford, R.L. (1980). Survival and disease patterns in C57BL/6J mice subjected to undernutrition. *Exp. Gerontol.* **15**, 237–258.
- Ciechanover, A. (2005). Proteolysis: from the lysosome to ubiquitin and the proteasome. *Nat. Rev. Mol. Cell Biol.* **6**, 79–87.
- Colman, R.J., Anderson, R.M., Johnson, S.C., Kastman, E.K., Kosmatka, K.J., Beasley, T.M., Allison, D.B., Cruzen, C., Simmons, H.A., Kemnitz, J.W., and Weindruch, R. (2009). Caloric restriction delays disease onset and mortality in rhesus monkeys. *Science* **325**, 201–204.
- Cuervo, A.M. (2008). Autophagy and aging: keeping that old broom working. *Trends Genet.* **24**, 604–612.
- Cuervo, A.M., Dice, J.F., and Knecht, E. (1997). A population of rat liver lysosomes responsible for the selective uptake and degradation of cytosolic proteins. *J. Biol. Chem.* **272**, 5606–5615.
- De Cabo, R., Cabello, R., Rios, M., López-Lluch, G., Ingram, D.K., Lane, M.A., and Navas, P. (2004). Calorie restriction attenuates age-related alterations in the plasma membrane antioxidant system in rat liver. *Exp. Gerontol.* **39**, 297–304.
- DeBalsi, K.L., Wong, K.E., Koves, T.R., Slentz, D.H., Seiler, S.E., Wittmann, A.H., Ilkayeva, O.R., Stevens, R.D., Perry, C.G.R., Lark, D.S., et al. (2014). Targeted metabolomics connects thioredoxin-interacting protein (TXNIP) to mitochondrial fuel selection and regulation of specific oxidoreductase enzymes in skeletal muscle. *J. Biol. Chem.* **289**, 8106–8120.
- Duffy, P.H., Feuers, R.J., Leakey, J.A., Nakamura, K., Turturro, A., and Hart, R.W. (1989). Effect of chronic caloric restriction on physiological variables related to energy metabolism in the male Fischer 344 rat. *Mech. Ageing Dev.* **48**, 117–133.
- Fernandes, G., Yunis, E.J., and Good, R.A. (1976). Influence of diet on survival of mice. *Proc. Natl. Acad. Sci. USA* **73**, 1279–1283.
- Figuroa, C.D., and Taberner, P.V. (1994). Pancreatic islet hypertrophy in spontaneous maturity onset obese-diabetic CBA/Ca mice. *Int. J. Biochem.* **26**, 1299–1303.
- Flegal, K.M., Kit, B.K., Orpana, H., and Graubard, B.I. (2013). Association of all-cause mortality with overweight and obesity using standard body mass index categories: a systematic review and meta-analysis. *JAMA* **309**, 71–82.
- Flurkey, K., Papaconstantinou, J., Miller, R.A., and Harrison, D.E. (2001). Lifespan extension and delayed immune and collagen aging in mutant mice with defects in growth hormone production. *Proc. Natl. Acad. Sci. USA* **98**, 6736–6741.
- Flurkey, K., Papaconstantinou, J., and Harrison, D.E. (2002). The Snell dwarf mutation Pit1(dw) can increase life span in mice. *Mech. Ageing Dev.* **123**, 121–130.
- Fontana, L., and Partridge, L. (2015). Promoting health and longevity through diet: from model organisms to humans. *Cell* **161**, 106–118.
- Fontana, L., Kennedy, B.K., Longo, V.D., Seals, D., and Melov, S. (2014). Medical research: treat ageing. *Nature* **511**, 405–407.
- Fontana, L., Villareal, D.T., Das, S.K., Smith, S.R., Meydani, S.N., Pittas, A.G., Klein, S., Bhapkar, M., Rochon, J., Ravussin, E., and Holloszy, J.O.; CALERIE Study Group (2016). Effects of 2-year calorie restriction on circulating levels of IGF-1, IGF-binding proteins and cortisol in nonobese men and women: a randomized clinical trial. *Ageing Cell* **15**, 22–27.
- Forster, M.J., Morris, P., and Sohal, R.S. (2003). Genotype and age influence the effect of caloric intake on mortality in mice. *FASEB J.* **17**, 690–692.
- Gomes, L.C., Di Benedetto, G., and Scorrano, L. (2011). During autophagy mitochondria elongate, are spared from degradation and sustain cell viability. *Nat. Cell Biol.* **13**, 589–598.
- Gomes, A.P., Price, N.L., Ling, A.J., Moslehi, J.J., Montgomery, M.K., Rajman, L., White, J.P., Teodoro, J.S., Wrann, C.D., Hubbard, B.P., et al. (2013). Declining NAD(+) induces a pseudohypoxic state disrupting nuclear-mitochondrial communication during aging. *Cell* **155**, 1624–1638.
- Goodrick, C.L., Ingram, D.K., Reynolds, M.A., Freeman, J.R., and Cider, N. (1990). Effects of intermittent feeding upon body weight and lifespan in inbred mice: interaction of genotype and age. *Mech. Ageing Dev.* **55**, 69–87.
- Grabowski, D.C., and Ellis, J.E. (2001). High body mass index does not predict mortality in older people: analysis of the Longitudinal Study of Aging. *J. Am. Geriatr. Soc.* **49**, 968–979.
- Gregg, S.Q., Gutiérrez, V., Robinson, A.R., Woodell, T., Nakao, A., Ross, M.A., Michalopoulos, G.K., Rigatti, L., Rothermel, C.E., Kamileri, I., et al. (2012). A mouse model of accelerated liver aging caused by a defect in DNA repair. *Hepatology* **55**, 609–621.
- Gross, L., and Dreyfuss, Y. (1984). Reduction in the incidence of radiation-induced tumors in rats after restriction of food intake. *Proc. Natl. Acad. Sci. USA* **81**, 7596–7598.
- Guan, K.L., and Xiong, Y. (2011). Regulation of intermediary metabolism by protein acetylation. *Trends Biochem. Sci.* **36**, 108–116.
- Guevara-Aguirre, J., Balasubramanian, P., Guevara-Aguirre, M., Wei, M., Madia, F., Cheng, C.W., Hwang, D., Martin-Montalvo, A., Saavedra, J., Ingles, S., et al. (2011). Growth hormone receptor deficiency is associated with a major reduction in pro-aging signaling, cancer, and diabetes in humans. *Sci. Transl. Med.* **3**, 70ra13.
- Hansen, M., Chandra, A., Mitic, L.L., Onken, B., Driscoll, M., and Kenyon, C. (2008). A role for autophagy in the extension of lifespan by dietary restriction in *C. elegans*. *PLoS Genet.* **4**, e24.
- Hara, T., Nakamura, K., Matsui, M., Yamamoto, A., Nakahara, Y., Suzuki-Migishima, R., Yokoyama, M., Mishima, K., Saito, I., Okano, H., and Mizushima, N. (2006). Suppression of basal autophagy in neural cells causes neurodegenerative disease in mice. *Nature* **441**, 885–889.
- Harper, J.M., Leathers, C.W., and Austad, S.N. (2006). Does caloric restriction extend life in wild mice? *Ageing Cell* **5**, 441–449.
- Harrison, D.E., and Archer, J.R. (1987). Genetic differences in effects of food restriction on aging in mice. *J. Nutr.* **117**, 376–382.
- Harrison, D.E., Strong, R., Sharp, Z.D., Nelson, J.F., Astle, C.M., Flurkey, K., Nadon, N.L., Wilkinson, J.E., Frenkel, K., Carter, C.S., et al. (2009). Rapamycin fed late in life extends lifespan in genetically heterogeneous mice. *Nature* **460**, 392–395.
- Harrison, D.E., Strong, R., Allison, D.B., Ames, B.N., Astle, C.M., Atamna, H., Fernandez, E., Flurkey, K., Javors, M.A., Nadon, N.L., et al. (2014). Acarbose, 17- α -estradiol, and nordihydroguaiaretic acid extend mouse lifespan preferentially in males. *Ageing Cell* **13**, 273–282.
- Hine, C., Harputlugil, E., Zhang, Y., Ruckenstein, C., Lee, B.C., Brace, L., Longchamp, A., Treviño-Villarreal, J.H., Mejia, P., Ozaki, C.K., et al. (2015). Endogenous hydrogen sulfide production is essential for dietary restriction benefits. *Cell* **160**, 132–144.
- Hsieh, C.C., DeFord, J.H., Flurkey, K., Harrison, D.E., and Papaconstantinou, J. (2002). Effects of the Pit1 mutation on the insulin signaling pathway: implications on the longevity of the long-lived Snell dwarf mouse. *Mech. Ageing Dev.* **123**, 1245–1255.
- Ikeno, Y., Hubbard, G.B., Lee, S., Dube, S.M., Flores, L.C., Roman, M.G., and Bartke, A. (2013). Do Ames dwarf and calorie-restricted mice share common effects on age-related pathology? *Pathobiol. Aging Age Relat. Dis.* **3**, <http://dx.doi.org/10.3402/pba.v3i0.20833>.
- Kabeya, Y., Mizushima, N., Ueno, T., Yamamoto, A., Kirisako, T., Noda, T., Kominami, E., Ohsumi, Y., and Yoshimori, T. (2000). LC3, a mammalian homologue of yeast Apg8p, is localized in autophagosomal membranes after processing. *EMBO J.* **19**, 5720–5728.
- Kaushik, S., and Cuervo, A.M. (2015). Proteostasis and aging. *Nat. Med.* **21**, 1406–1415.
- Khraiwesh, H., López-Domínguez, J.A., López-Lluch, G., Navas, P., de Cabo, R., Ramsey, J.J., Villalba, J.M., and González-Reyes, J.A. (2013). Alterations of ultrastructural and fission/fusion markers in hepatocyte mitochondria from mice following calorie restriction with different dietary fats. *J. Gerontol. A Biol. Sci. Med. Sci.* **68**, 1023–1034.
- Khraiwesh, H., López-Domínguez, J.A., Fernández del Río, L., Gutierrez-Casado, E., López-Lluch, G., Navas, P., de Cabo, R., Ramsey, J.J., Burón,

- M.I., Villalba, J.M., and González-Reyes, J.A. (2014). Mitochondrial ultrastructure and markers of dynamics in hepatocytes from aged, calorie restricted mice fed with different dietary fats. *Exp. Gerontol.* *56*, 77–88.
- Kirkwood, T.B. (2002). Evolution of ageing. *Mech. Ageing Dev.* *123*, 737–745.
- Kirkwood, T.B., and Shanley, D.P. (2005). Food restriction, evolution and ageing. *Mech. Ageing Dev.* *126*, 1011–1016.
- Kritchevsky, D. (2002). Caloric restriction and experimental carcinogenesis. *Hybrid. Hybridomics* *21*, 147–151.
- Kuhla, A., Hahn, S., Butschkau, A., Lange, S., Wree, A., and Vollmar, B. (2014). Lifelong Caloric Restriction Reprograms Hepatic Fat Metabolism in Mice. *J. Gerontol. A Biol. Sci. Med. Sci.* *69*, 915–922.
- Lane, M.A., Ball, S.S., Ingram, D.K., Cutler, R.G., Engel, J., Read, V., and Roth, G.S. (1995). Diet restriction in rhesus monkeys lowers fasting and glucose-stimulated glucoregulatory end points. *Am. J. Physiol.* *268*, E941–E948.
- Liao, C.-Y., Rikke, B.A., Johnson, T.E., Diaz, V., and Nelson, J.F. (2010). Genetic variation in the murine lifespan response to dietary restriction: from life extension to life shortening. *Aging Cell* *9*, 92–95.
- Liao, C.-Y., Rikke, B.A., Johnson, T.E., Gelfond, J.A.L., Diaz, V., and Nelson, J.F. (2011). Fat maintenance is a predictor of the murine lifespan response to dietary restriction. *Aging Cell* *10*, 629–639.
- Longo, V.D., Antebi, A., Bartke, A., Barzilai, N., Brown-Borg, H.M., Caruso, C., Curiel, T.J., de Cabo, R., Franceschi, C., Gems, D., et al. (2015). Interventions to Slow Aging in Humans: Are We Ready? *Aging Cell* *14*, 497–510.
- López-Lluch, G., Hunt, N., Jones, B., Zhu, M., Jamieson, H., Hilmer, S., Cascajo, M.V., Allard, J., Ingram, D.K., Navas, P., and de Cabo, R. (2006). Calorie restriction induces mitochondrial biogenesis and bioenergetic efficiency. *Proc. Natl. Acad. Sci. USA* *103*, 1768–1773.
- Madrigal-Matute, J., and Cuervo, A.M. (2016). Regulation of Liver Metabolism by Autophagy. *Gastroenterology* *150*, 328–339.
- Martin-Montalvo, A., Mercken, E.M., Mitchell, S.J., Palacios, H.H., Mote, P.L., Scheibye-Knudsen, M., Gomes, A.P., Ward, T.M., Minor, R.K., Blouin, M.J., et al. (2013). Metformin improves healthspan and lifespan in mice. *Nat. Commun.* *4*, 2192.
- Masoro, E.J. (1990). Assessment of nutritional components in prolongation of life and health by diet. *Proc. Soc. Exp. Biol. Med.* *193*, 31–34.
- Masternak, M.M., Panici, J.A., Bonkowski, M.S., Hughes, L.F., and Bartke, A. (2009). Insulin sensitivity as a key mediator of growth hormone actions on longevity. *J. Gerontol. A Biol. Sci. Med. Sci.* *64*, 516–521.
- Mattison, J.A., Roth, G.S., Beasley, T.M., Tilmont, E.M., Handy, A.M., Herbert, R.L., Longo, D.L., Allison, D.B., Young, J.E., Bryant, M., et al. (2012). Impact of caloric restriction on health and survival in rhesus monkeys from the NIA study. *Nature* *489*, 318–321.
- McCay, C.M., Crowell, M.F., and Maynard, L.A. (1935). The effect of retarded growth upon the length of life span and upon the ultimate body size. *J. Nutr.* *10*, 63–79.
- Merkwirth, C., Dargazanli, S., Tatsuta, T., Geimer, S., Löwer, B., Wunderlich, F.T., von Kleist-Retzow, J.C., Waisman, A., Westermann, B., and Langer, T. (2008). Prohibitins control cell proliferation and apoptosis by regulating OPA1-dependent cristae morphogenesis in mitochondria. *Genes Dev.* *22*, 476–488.
- Miller, D.L., and Roth, M.B. (2007). Hydrogen sulfide increases thermotolerance and lifespan in *Caenorhabditis elegans*. *Proc. Natl. Acad. Sci. USA* *104*, 20618–20622.
- Miller, R.A., Harrison, D.E., Astle, C.M., Baur, J.A., Boyd, A.R., de Cabo, R., Fernandez, E., Flurkey, K., Javors, M.A., Nelson, J.F., et al. (2011). Rapamycin, but not resveratrol or simvastatin, extends life span of genetically heterogeneous mice. *J. Gerontol. A Biol. Sci. Med. Sci.* *66*, 191–201.
- Miller, R.A., Harrison, D.E., Astle, C.M., Fernandez, E., Flurkey, K., Han, M., Javors, M.A., Li, X., Nadon, N.L., Nelson, J.F., et al. (2014). Rapamycin-mediated lifespan increase in mice is dose and sex dependent and metabolically distinct from dietary restriction. *Aging Cell* *13*, 468–477.
- Milman, S., Atzmon, G., Huffman, D.M., Wan, J., Crandall, J.P., Cohen, P., and Barzilai, N. (2014). Low insulin-like growth factor-1 level predicts survival in humans with exceptional longevity. *Aging Cell* *13*, 769–771.
- Mitchell, S.E., Delville, C., Konstantopoulos, P., Deros, D., Green, C.L., Chen, L., Han, J.D., Wang, Y., Promislow, D.E., Douglas, A., et al. (2015a). The effects of graded levels of calorie restriction: III. Impact of short term calorie and protein restriction on mean daily body temperature and torpor use in the C57BL/6 mouse. *Oncotarget* *6*, 18314–18337.
- Mitchell, S.E., Delville, C., Konstantopoulos, P., Hurst, J., Deros, D., Green, C., Chen, L., Han, J.J., Wang, Y., Promislow, D.E., et al. (2015b). The effects of graded levels of calorie restriction: II. Impact of short term calorie and protein restriction on circulating hormone levels, glucose homeostasis and oxidative stress in male C57BL/6 mice. *Oncotarget* *6*, 23213–23237.
- Moreschi, C. (1909). Beziehungen zwischen ernährung und tumorwachstum. *Zeitschrift f Immunitätsforschung Originale* *2*, 651–675.
- Moscovitz, O., Ben-Nissan, G., Fainer, I., Pollack, D., Mizrahi, L., and Sharon, M. (2015). The Parkinson's-associated protein DJ-1 regulates the 20S proteasome. *Nat. Commun.* *6*, 6609.
- Murtagh-Mark, C.M., Reiser, K.M., Harris, R., Jr., and McDonald, R.B. (1995). Source of dietary carbohydrate affects life span of Fischer 344 rats independent of caloric restriction. *J. Gerontol. A Biol. Sci. Med. Sci.* *50*, B148–B154.
- Nisoli, E., Tonello, C., Cardile, A., Cozzi, V., Bracale, R., Tedesco, L., Falcone, S., Valerio, A., Cantoni, O., Clementi, E., et al. (2005). Calorie restriction promotes mitochondrial biogenesis by inducing the expression of eNOS. *Science* *310*, 314–317.
- Olzmann, J.A., and Chin, L.S. (2008). Parkin-mediated K63-linked polyubiquitination: a signal for targeting misfolded proteins to the aggresome-autophagy pathway. *Autophagy* *4*, 85–87.
- Osborne, T.B., Mendel, L.B., and Ferry, E.L. (1917). The Effect of Retardation of Growth Upon the Breeding Period and Duration of Life of Rats. *Science* *45*, 294–295.
- Pearson, K.J., Baur, J.A., Lewis, K.N., Peshkin, L., Price, N.L., Labinskyy, N., Swindell, W.R., Kamara, D., Minor, R.K., Perez, E., et al. (2008a). Resveratrol delays age-related deterioration and mimics transcriptional aspects of dietary restriction without extending life span. *Cell Metab.* *8*, 157–168.
- Pearson, K.J., Lewis, K.N., Price, N.L., Chang, J.W., Perez, E., Cascajo, M.V., Tamashiro, K.L., Poovala, S., Csiszar, A., Ungvari, Z., et al. (2008b). Nrf2 mediates cancer protection but not longevity induced by caloric restriction. *Proc. Natl. Acad. Sci. USA* *105*, 2325–2330.
- Qiao, S., Dennis, M., Song, X., Vadysirisack, D.D., Salunke, D., Nash, Z., Yang, Z., Liesa, M., Yoshioka, J., Matsuzawa, S., et al. (2015). A REDD1/TXNIP pro-oxidant complex regulates ATG4B activity to control stress-induced autophagy and sustain exercise capacity. *Nat. Commun.* *6*, 7014.
- Qiu, X., Brown, K., Hirsche, M.D., Verdin, E., and Chen, D. (2010). Calorie restriction reduces oxidative stress by SIRT3-mediated SOD2 activation. *Cell Metab.* *12*, 662–667.
- Rikke, B.A., and Johnson, T.E. (2007). Physiological genetics of dietary restriction: uncoupling the body temperature and body weight responses. *Am. J. Physiol. Regul. Integr. Comp. Physiol.* *293*, R1522–R1527.
- Rikke, B.A., Yerg, J.E., 3rd, Battaglia, M.E., Nagy, T.R., Allison, D.B., and Johnson, T.E. (2003). Strain variation in the response of body temperature to dietary restriction. *Mech. Ageing Dev.* *124*, 663–678.
- Rikke, B.A., Liao, C.Y., McQueen, M.B., Nelson, J.F., and Johnson, T.E. (2010). Genetic dissection of dietary restriction in mice supports the metabolic efficiency model of life extension. *Exp. Gerontol.* *45*, 691–701.
- Rous, P. (1914). The influence of diet on transplanted and spontaneous tumors. *J. Exp. Med.* *20*, 433–451.
- Sadagurski, M., Landeryou, T., Blandino-Rosano, M., Cady, G., Elghazi, L., Meister, D., See, L., Bartke, A., Bernal-Mizrahi, E., and Miller, R.A. (2014). Long-lived crowded-litter mice exhibit lasting effects on insulin sensitivity and energy homeostasis. *Am. J. Physiol. Endocrinol. Metab.* *306*, E1305–E1314.
- Schneider, J.L., Suh, Y., and Cuervo, A.M. (2014). Deficient chaperone-mediated autophagy in liver leads to metabolic dysregulation. *Cell Metab.* *20*, 417–432.

- Schwer, B., Eckersdorff, M., Li, Y., Silva, J.C., Fermin, D., Kurtev, M.V., Giallourakis, C., Comb, M.J., Alt, F.W., and Lombard, D.B. (2009). Calorie restriction alters mitochondrial protein acetylation. *Aging Cell* 8, 604–606.
- Shang, Z., Lu, C., Chen, S., Hua, L., and Qian, R. (2012). Effect of H₂S on the circadian rhythm of mouse hepatocytes. *Lipids Health Dis.* 11, 23.
- Sharples, A.P., Hughes, D.C., Deane, C.S., Saini, A., Selman, C., and Stewart, C.E. (2015). Longevity and skeletal muscle mass: the role of IGF signalling, the sirtuins, dietary restriction and protein intake. *Aging Cell* 14, 511–523.
- Sheth, S.S., Castellani, L.W., Chari, S., Wagg, C., Thippavong, C.K., Bodnar, J.S., Tontonoz, P., Attie, A.D., Lopaschuk, G.D., and Lusis, A.J. (2005). Thioredoxin-interacting protein deficiency disrupts the fasting-feeding metabolic transition. *J. Lipid Res.* 46, 123–134.
- Shimokawa, I., Komatsu, T., Hayashi, N., Kim, S.E., Kawata, T., Park, S., Hayashi, H., Yamaza, H., Chiba, T., and Mori, R. (2015). The life-extending effect of dietary restriction requires Foxo3 in mice. *Aging Cell* 14, 707–709.
- Singh, R., Kaushik, S., Wang, Y., Xiang, Y., Novak, I., Komatsu, M., Tanaka, K., Cuervo, A.M., and Czaja, M.J. (2009). Autophagy regulates lipid metabolism. *Nature* 458, 1131–1135.
- Soare, A., Cangemi, R., Omodei, D., Holloszy, J.O., and Fontana, L. (2011). Long-term calorie restriction, but not endurance exercise, lowers core body temperature in humans. *Aging (Albany, N.Y.)* 3, 374–379.
- Solon-Biet, S.M., Mitchell, S.J., Coogan, S.C., Cogger, V.C., Gokarn, R., McMahon, A.C., Raubenheimer, D., de Cabo, R., Simpson, S.J., and Le Couteur, D.G. (2015). Dietary Protein to Carbohydrate Ratio and Caloric Restriction: Comparing Metabolic Outcomes in Mice. *Cell Rep.* 11, 1529–1534.
- Speakman, J.R., and Mitchell, S.E. (2011). Caloric restriction. *Mol. Aspects Med.* 32, 159–221.
- Strong, R., Miller, R.A., Astle, C.M., Floyd, R.A., Flurkey, K., Hensley, K.L., Javors, M.A., Leeuwenburgh, C., Nelson, J.F., Ongini, E., et al. (2008). NORDIHYDROGUAIARETIC ACID AND ASPIRIN INCREASE LIFESPAN OF GENETICALLY HETEROGENEOUS MALE MICE. *Aging Cell* 7, 641–650.
- Strong, R., Miller, R.A., Astle, C.M., Baur, J.A., de Cabo, R., Fernandez, E., Guo, W., Javors, M., Kirkland, J.L., Nelson, J.F., et al. (2013). Evaluation of resveratrol, green tea extract, curcumin, oxaloacetic acid, and medium-chain triglyceride oil on life span of genetically heterogeneous mice. *J. Gerontol. A Biol. Sci. Med. Sci.* 68, 6–16.
- Sun, L.Y., Spong, A., Swindell, W.R., Fang, Y., Hill, C., Huber, J.A., Boehm, J.D., Westbrook, R., Salvatori, R., and Bartke, A. (2013). Growth hormone-releasing hormone disruption extends lifespan and regulates response to caloric restriction in mice. *eLife* 2, e01098.
- Tan, J.M., Wong, E.S., Kirkpatrick, D.S., Pletnikova, O., Ko, H.S., Tay, S.P., Ho, M.W., Troncoso, J., Gygi, S.P., Lee, M.K., et al. (2008). Lysine 63-linked ubiquitination promotes the formation and autophagic clearance of protein inclusions associated with neurodegenerative diseases. *Hum. Mol. Genet.* 17, 431–439.
- Tannenbaum, A. (1940). The initiation and growth of tumors. Introduction. I. Effects of underfeeding. *Am. J. Cancer* 38, 335–350.
- Tauriainen, E., Luostarinen, M., Martonen, E., Finckenberg, P., Kovalainen, M., Huotari, A., Herzig, K.H., Lecklin, A., and Mervaala, E. (2011). Distinct effects of calorie restriction and resveratrol on diet-induced obesity and Fatty liver formation. *J. Nutr. Metab.* 2011, 525094.
- Turturro, A., and Hart, R.W. (1991). Longevity-assurance mechanisms and caloric restriction. *Ann. N Y Acad. Sci.* 621, 363–372.
- Turturro, A., Duffy, P., Hass, B., Kodell, R., and Hart, R. (2002). Survival characteristics and age-adjusted disease incidences in C57BL/6 mice fed a commonly used cereal-based diet modulated by dietary restriction. *J. Gerontol. A Biol. Sci. Med. Sci.* 57, B379–B389.
- Twig, G., Elorza, A., Molina, A.J., Mohamed, H., Wikstrom, J.D., Walzer, G., Stiles, L., Haigh, S.E., Katz, S., Las, G., et al. (2008). Fission and selective fusion govern mitochondrial segregation and elimination by autophagy. *EMBO J.* 27, 433–446.
- Weindruch, R., and Sohal, R.S. (1997). Seminars in medicine of the Beth Israel Deaconess Medical Center. Caloric intake and aging. *N. Engl. J. Med.* 337, 986–994.
- Weindruch, R.H., Kristie, J.A., Cheney, K.E., and Walford, R.L. (1979). Influence of controlled dietary restriction on immunologic function and aging. *Fed. Proc.* 38, 2007–2016.
- Weindruch, R., Walford, R.L., Fligiel, S., and Guthrie, D. (1986). The retardation of aging in mice by dietary restriction: longevity, cancer, immunity and lifetime energy intake. *J. Nutr.* 116, 641–654.
- Yang, G., Zhao, K., Ju, Y., Mani, S., Cao, Q., Puukila, S., Khaper, N., Wu, L., and Wang, R. (2013). Hydrogen sulfide protects against cellular senescence via S-sulfhydration of Keap1 and activation of Nrf2. *Antioxid. Redox Signal.* 18, 1906–1919.
- Yang, L., Licastro, D., Cava, E., Veronese, N., Spelta, F., Rizza, W., Bertozzi, B., Villareal, D.T., Hotamisligil, G.S., Holloszy, J.O., and Fontana, L. (2016). Long-Term Calorie Restriction Enhances Cellular Quality-Control Processes in Human Skeletal Muscle. *Cell Rep.* 14, 422–428.
- Yuan, R., Tsaih, S.-W., Petkova, S.B., Marin de Evsikova, C., Xing, S., Marion, M.A., Bogue, M.A., Mills, K.D., Peters, L.L., Bult, C.J., et al. (2009). Aging in inbred strains of mice: study design and interim report on median lifespans and circulating IGF1 levels. *Aging Cell* 8, 277–287.
- Zee, R.S., Yoo, C.B., Pimentel, D.R., Perlman, D.H., Burgoyne, J.R., Hou, X., McComb, M.E., Costello, C.E., Cohen, R.A., and Bachschmid, M.M. (2010). Redox regulation of sirtuin-1 by S-glutathiolation. *Antioxid. Redox Signal.* 13, 1023–1032.
- Zhang, C., and Cuervo, A.M. (2008). Restoration of chaperone-mediated autophagy in aging liver improves cellular maintenance and hepatic function. *Nat. Med.* 14, 959–965.